iScience

CellPress
OPEN ACCESS

Article

Schlafen-5 inhibits LINE-1 retrotransposition

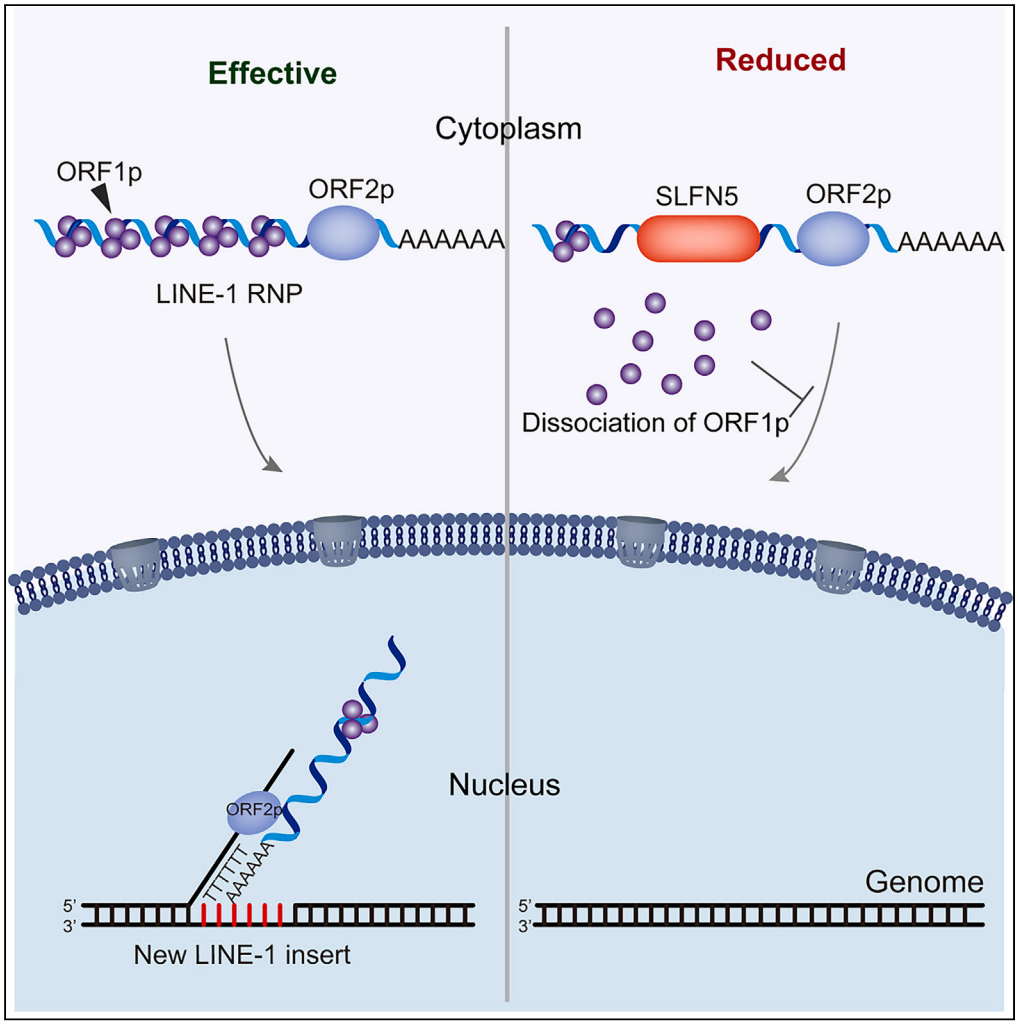

Jiwei Ding, Shujie Wang, Qipeng Liu, ..., Jinming Zhou, Shan Cen, Xiaoyu Li

zhoujinming@zjnu.edu.cn (J.Z.)
shancen@imb.pumc.edu.cn (S.C.)
lixiaoyu@imb.pumc.edu.cn (X.L.)

Highlights

SLFN5 inhibits LINE-1 retrotransposition

SLFN5 disrupts LINE-1 ribonucleoprotein particle (RNP) formation

SLFN5 interferes with LINE-1 RNP nuclear import

Helicase activity of SLFN5 is required for restricting LINE-1 retrotransposition

Ding et al., iScience *26*, 107968
October 20, 2023
https://doi.org/10.1016/j.isci.2023.107968

iScience

CellPress
OPEN ACCESS

Article

Schlafen-5 inhibits LINE-1 retrotransposition

Jiwei Ding,[1,5] Shujie Wang,[1,5] Qipeng Liu,[1,5] Yuqing Duan,[1] Tingting Cheng,[1] Zhongjie Ye,[1] Zhanding Cui,[1] Ao Zhang,[1] Qiuyu Liu,[1] Zixiong Zhang,[1] Ning Zhang,[1] Qian Liu,[1] Ni An,[1] Jianyuan Zhao,[1] Dongrong Yi,[1] Quanjie Li,[1] Jing Wang,[1] Yongxin Zhang,[1] Ling Ma,[1] Saisai Guo,[1] Jinhui Wang,[2] Chen Liang,[3] Jinming Zhou,[4,*] Shan Cen,[1,*] and Xiaoyu Li[1,6,*]

SUMMARY

Long interspersed element 1 (LINE-1) is the only currently known active autonomous transposon in humans, and its retrotransposition may cause deleterious effects on the structure and function of host cell genomes and result in sporadic genetic diseases. Host cells therefore developed defense strategies to restrict LINE-1 mobilization. In this study, we demonstrated that IFN-inducible Schlafen5 (SLFN5) inhibits LINE-1 retrotransposition. Mechanistic studies revealed that SLFN5 interrupts LINE-1 ribonucleoprotein particle (RNP) formation, thus diminishing nuclear entry of the LINE-1 RNA template and subsequent LINE-1 cDNA production. The ability of SLFN5 to bind to LINE-1 RNA and the involvement of the helicase domain of SLFN5 in its inhibitory activity suggest a mechanism that SLFN5 binds to LINE-1 RNA followed by dissociation of ORF1p through its helicase activity, resulting in impaired RNP formation. These data highlight a new mechanism of host cells to restrict LINE-1 mobilization.

INTRODUCTION

LINE-1 is the only currently known active autonomous transposon in humans, with an estimated 500,000 copies representing 17% of the human genome.[1] It is approximately 6,000 nucleotides in length and belongs to a non-LTR retrotransposon. LINE-1 encodes a bicistronic RNA transcript that is translated into a 40-kDa RNA-binding protein ORF1p with RNA-binding and nucleic acid chaperone activities and a 150-kDa protein ORF2p with endonuclease and reverse transcriptase (RT) activities.[2] Both ORF1p and ORF2p proteins show a strong *cis*-preference,[3] and they associate with LINE-1 RNA to form a ribonucleoprotein particle (RNP). RNP is then gained access into the nucleus, where LINE-1 RNA is reverse transcribed into cDNA, which is subsequently incorporated into the host genome through a process termed target-primed reverse transcription (TPRT).[4,5] Recently, a primate-specific open reading frame, ORF0, was found in the 5′UTR of LINE-1, which was shown to enhance LINE-1 mobility and contribute to retrotransposon-mediated diversity.[6,7]

The transposition of LINE-1 may cause genetic instability and induce dozens of genetic diseases.[8–12] LINE-1 RNA and protein overexpression is commonly considered a hallmark of human cancers.[12] To avoid the deleterious effects of LINE-1 transposition on the structure and function of the host genome, host cells developed multiple strategies to inhibit LINE-1. In normal human somatic cells, LINE-1 transposition is tightly controlled by several layers of mechanisms. One mechanism involves DNA methylation in the 5′-UTR promoter region of LINE-1, which suppresses LINE-1 RNA transcription.[13–15] Noncoding RNA (ncRNA)-based RNA interference machinery, including siRNA, miRNA and piRNA, is considered another controlling mechanism against transposable elements (TEs).[16–20] Additionally, in recent years, it has been reported that many interferon-inducible host proteins, such as APOBEC3 proteins, MOV10, SAMHD1, and ZAP, also have inhibitory activities against LINE-1 retrotransposition.[21–35] It is worth noting that most of these cellular factors also have antiretroviral activity, particularly anti-HIV-1 activity, suggesting that common mechanisms might be utilized by host cells to protect themselves from either extracellular or intracellular insults that share common biochemical features.

The Schlafen (SLFN) family consists of a set of type 1 interferon inducible proteins, which include ten murine and six human isoforms.[36,37] These proteins are characterized by a conserved putative AAA domain as well as a structure referred to as a "Slfn box" in their N-terminus, and longer SLFN proteins also possess a DNA/RNA helicase-like structure in their C-terminus.[36,38] Early studies showed that SLFN family proteins play important roles in immunocyte development[39–42] and in the regulation of tumorigenesis.[43–47] Interestingly, a number of recent studies have shown that SLFN family proteins, such as SLFN11 and SLFN13, exhibited potent anti-HIV-1 activity.[36,48] These works implicate that SLFN family proteins might possess restricting activity against LINE-1, as other anti-HIV host factors do.

[1]Institute of Medicinal Biotechnology, Chinese Academy of Medical Sciences & Peking Union Medical College, Beijing, China
[2]Peking Union Medical College Hospital, Chinese Academy of Medical Sciences & Peking Union Medical College, Beijing, China
[3]The Lady Davis Institute-Jewish General Hospital, Montreal, QC H3T 1E2, Canada
[4]Key Laboratory of the Ministry of Education for Advanced Catalysis Materials, Department of Chemistry, Zhejiang Normal University, 688 Yingbin Road, Jinhua 321004, China
[5]These authors contributed equally
[6]Lead contact
*Correspondence: zhoujinming@zjnu.edu.cn (J.Z.), shancen@imb.pumc.edu.cn (S.C.), lixiaoyu@imb.pumc.edu.cn (X.L.)
https://doi.org/10.1016/j.isci.2023.107968

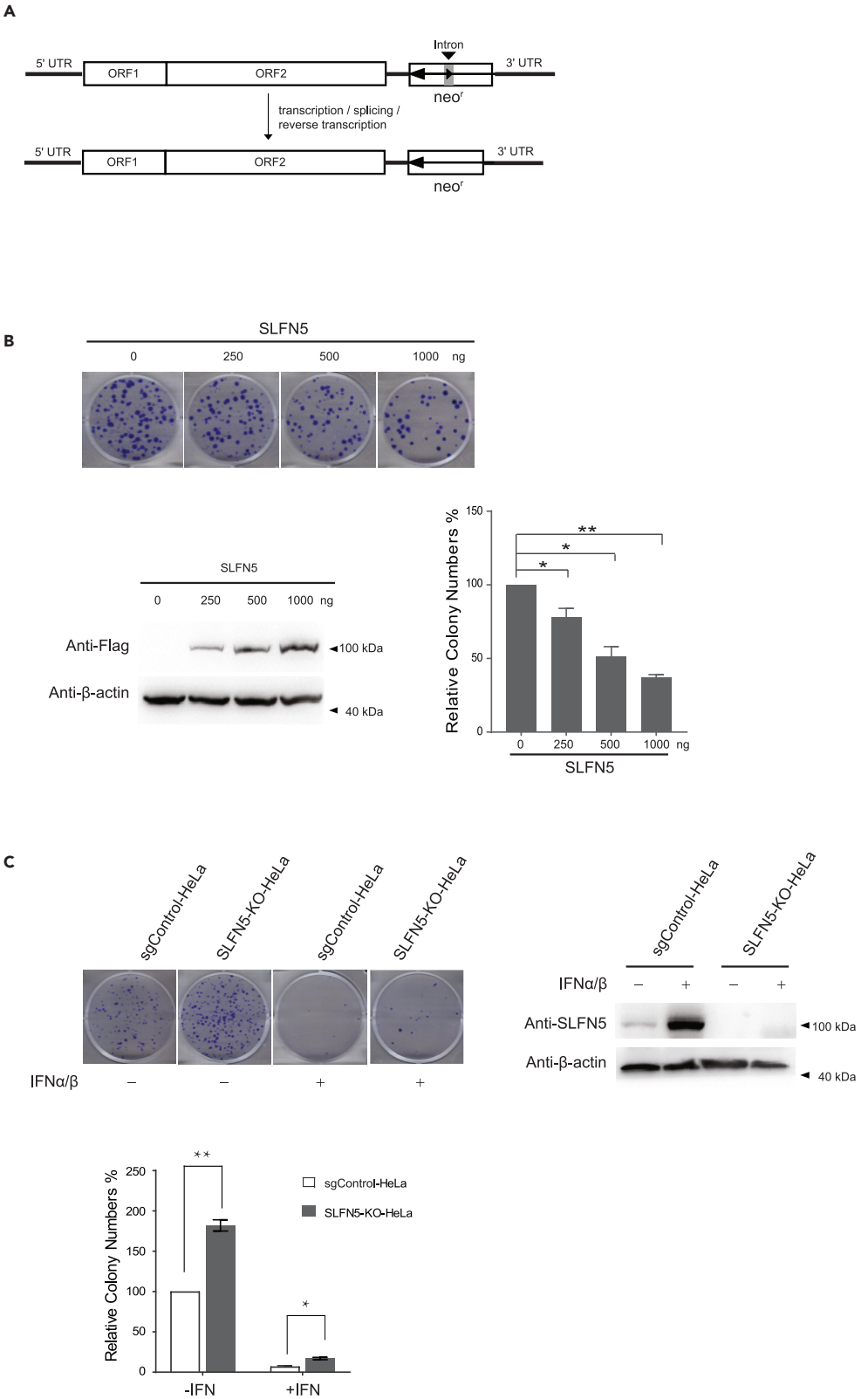
A
Intron
5' UTR
ORF1
ORF2
3' UTR
neor
transcription / splicing /
reverse transcription
5' UTR
ORF1
ORF2
3' UTR
neor
B
SLFN5
0
250
500
1000 ng
SLFN5
0 250 500 1000 ng
Anti-Flag
100 kDa
Anti-β-actin
40 kDa
Relative Colony Numbers %
150
100
50
0
**
*
*
0 250 500 1000 ng
SLFN5
C
sgControl-HeLa
SLFN5-KO-HeLa
sgControl-HeLa
SLFN5-KO-HeLa
IFNα/β – – + +
sgControl-HeLa
SLFN5-KO-HeLa
IFNα/β – + – +
Anti-SLFN5
100 kDa
Anti-β-actin
40 kDa
Relative Colony Numbers %
250
200
150
100
50
0
**
*
sgControl-HeLa
SLFN5-KO-HeLa
-IFN
+IFN

Figure 1. SLFN5 inhibits LINE-1 retrotransposition

(A) Schematic of the CMV-L1-neo^{RT} reporter and an overview of the LINE-1 retrotransposition assay. Following transcription from the 5′ UTR promoter of LINE-1, the intron in the neomycin resistance gene is removed. The intronless mRNA is then reverse transcribed into cDNA, which can produce a functional neomycin resistance mRNA.

(B) Overexpressing SLFN5 inhibited LINE-1 mobilization. HeLa cells were transfected with 1000 ng CMV-L1-neo^{RT} DNA and 250, 500, and 1000 ng SLFN5 plasmids, followed by retrotransposition assay. SLFN5 expression was monitored by Western blot using an anti-Flag probe. The colony numbers represent LINE-1 mobilization activity. Colonies were visualized with crystal violet staining. The data from three independent experiments are summarized in the bar graph.

(C) Depletion of SLFN5 enhances LINE-1 mobility. The SLFN5 knockout HeLa cell line (SLFN5-KO-HeLa) and control HeLa cells (sgControl-HeLa) were transfected with 1000 ng CMV-L1-neo^{RT} DNA followed by treatment with or without IFNα/β, and then a retrotransposition assay was performed. Endogenous SLFN5 was detected by an anti-SLFN5 probe. The data from three independent experiments are summarized in the bar graph. Throughout the figure, statistical significance was determined by unpaired two-tailed Student's *t* test. *$p < 0.05$; **$p < 0.01$.

SLFN5, one member of type III human SLFN family, has been reported to exhibit potent antitumor activity. In melanoma cell lines, SLFN5 knockdown resulted in increased anchorage-independent growth and invasion in three-dimensional collagen, implicating its function in the regulation of cell invasion.[44] In renal cell carcinoma (RCC) cells, SLFN5 also plays key roles in controlling motility and invasiveness. Furthermore, SLFN5 expression correlates with better overall survival in a large cohort of patients with RCC.[47] Given the close association between human cancer and increased expression of LINE-1, these studies implicate the potential role of SLFN5 in controlling LINE-1 activation.

In this study, we provided evidence that the SLFN5 protein effectively suppresses LINE-1 transposition by interfering with LINE-1 RNP formation and reducing LINE-1 RNA entry into the nucleus, thus inhibiting LINE-1 cDNA production. This work highlights a new mechanism for the host to negatively control the transposition of LINE-1, providing further protection to maintain genetic stability.

RESULTS

SLFN5 inhibits LINE-1 retrotransposition

To determine whether SLFN5 participated in the regulation of LINE-1 transposition, we employed a retrotransposition assay to evaluate the transposition efficiency of LINE-1 in the presence of SLFN5. A plasmid, CMV-L1-neo^{RT}, has an antisense neomycin resistance gene inserted between ORF2p and the 3′UTR of LINE-1, which is disrupted with an intron in the same transcription orientation as LINE-1 (Figure 1A) and driven by a CMV immediate-early promoter.[49] Such a design ensures that the resistance gene will only be produced from the reverse transcribed LINE-1 DNA in which the intron should have been removed during RNA splicing. Therefore, the number of G418-resistant cell colonies reflects the events of LINE-1 retrotransposition. We transfected CMV-L1-neo^{RT} DNA with or without the SLFN5-expressing plasmid into HeLa cells, followed by retrotransposition assay. We discovered that ectopic expression of SLFN5 diminished the number of G418-resistant HeLa colonies by ~20%, 40%, and 70% ($p < 0.05$) according to different SLFN5 expression levels (Figure 1B). We also used pDNA4.0-EGFP as a negative control to exclude any side effects of transfecting another plasmid with LINE-1. As expected, the colony number of EGFP+ expressing cells is similar to the colony number of control cells (Figure S1A). This result indicates that overexpression of SLFN5 specifically inhibits LINE-1 retrotransposition in a dose-dependent manner.

We next assessed the activity of endogenous SLFN5 against LINE-1 using a stable SLFN5 knockout (KO) cell line, SLFN5-KO-HeLa, in which SLFN5 alleles were knocked out (KO) using CRISPR-Cas9 genome editing. Indels introduced by sgRNA targeting were validated by Sanger sequencing (Figure S1B). We observed that the depletion of endogenous SLFN5 resulted in an increase in the number of G418-resistant HeLa colonies by ~2-fold ($p < 0.05$) compared to control cells (Figure 1C), providing further evidence supporting the function of SLFN5 to inhibit LINE-1 transposition. Of note, while early studies showed that SLFN5 and other members of this family play important roles in the proliferation and anchorage-independent growth of some tumor cell lines, we did not observe any significant effect of transient expression of SLFN5 on the viability of HeLa cells (Figure S1C). This most likely excludes the possibility that the SLFN5-mediated inhibitory effect on LINE-1 retrotransposition was derived from its cellular cytotoxicity.

IFN treatment was shown to efficiently suppress LINE-1 expression, and it is interesting to understand whether SLFN5, as an interferon-inducible protein, also contributes to the inhibition by IFN. In agreement with early studies, IFNα/β treatment significantly induced the expression of endogenous SLFN5 in HeLa cells at a level comparable to that of ectopic SLFN5 (Figure S1D) and inhibited LINE-1 transposition by ~ 10-fold (Figure 1C). It is worth noting that under the same conditions of IFNα/β treatment, the colonies arising from SLFN5-KO cells were ~ 2-fold greater than those arising from control cells (Figure 1C). Taken together, these results demonstrate an inhibitory effect of SLFN5 upon LINE-1 retrotransposition and suggest its role in IFN-mediated inhibition of LINE-1 retrotransposition.

SLFN5 inhibits LTR retrotransposon IAP

To explore the specificity of SLFN-mediated inhibition on retrotransposition, we next determined whether SLFN5 restricts other retrotransposons, such as LTR retrotransposons. To this end, we further assessed the activity of SLFN5 against MusD and IAP, two representative murine long-term repeat (LTR) retrotransposons, using two constructs, MusD-neo^{TNF} and IAP-neo. Both carry the neomycin resistance selection marker in a similar way as CMV-L1-neo^{RT} (Figure 2A) and are able to generate G418-resistant cell colonies once retrotransposition occurs. The retrotransposition assay results showed that SLFN5 expression had no effect on the colony number of the cells transfected with either MusD-neo^{TNF} or pcDNA3.1 DNA. The latter was used as a control to monitor any nonspecific effect of SLFN5 on neomycin phosphotransferase expression or activity. Interestingly, in contrast to the case of MuSD, SLFN5 exerted an even more potent inhibitory activity on IAP than on

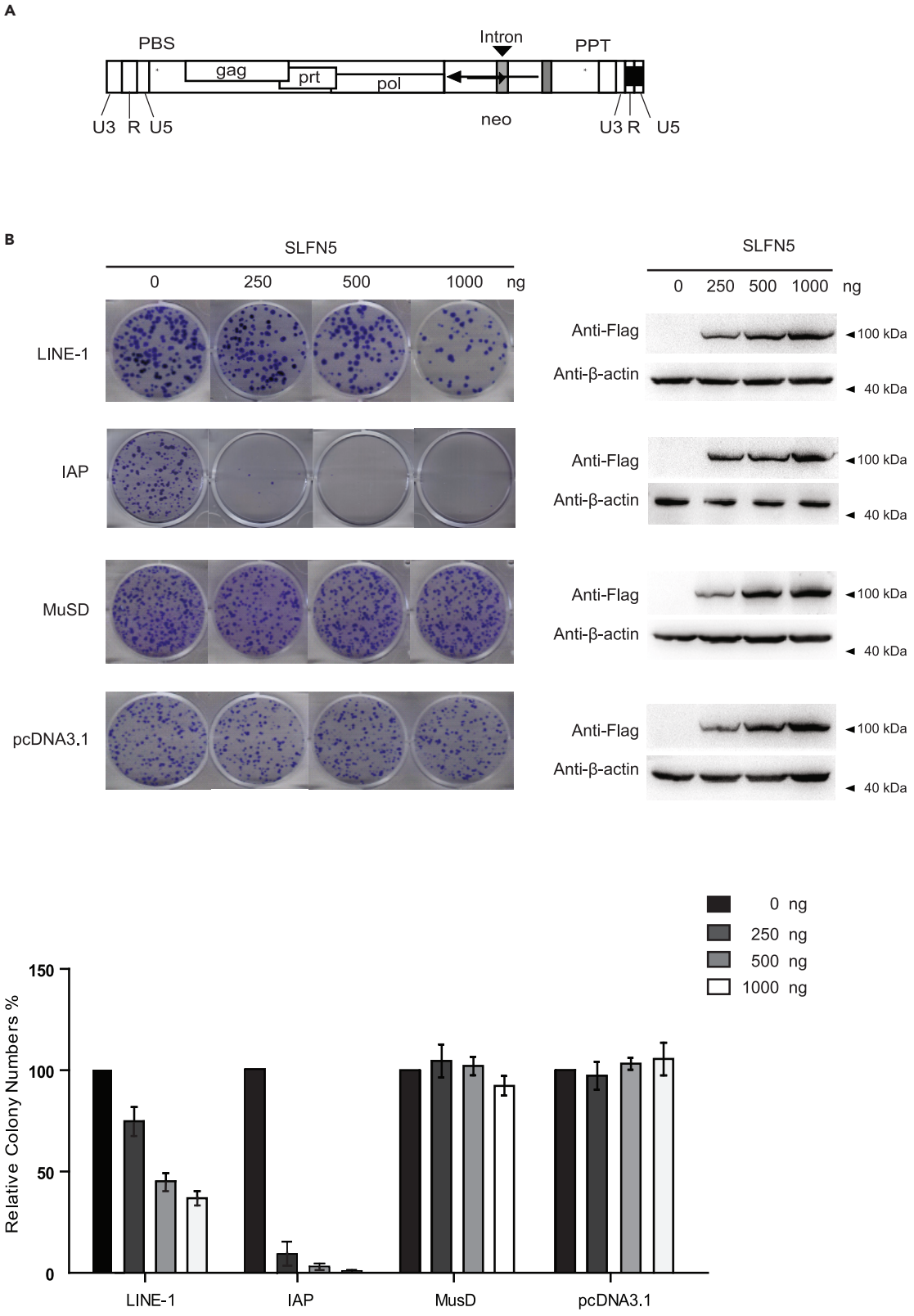
A
PBS
gag
prt
pol
Intron
PPT
neo
U3 R U5
U3 R U5
B
SLFN5
0 250 500 1000 ng
LINE-1
IAP
MuSD
pcDNA3.1
Anti-Flag
Anti-β-actin
100 kDa
40 kDa
0 ng
250 ng
500 ng
1000 ng
Relative Colony Numbers %
150
100
50
0
LINE-1
IAP
MusD
pcDNA3.1

Figure 2. SLFN5 specifically inhibits LINE-1

(A) Schematics of the MusD-neo^{TNF} and IAP-neo^{TNF} reporter.

(B) G418 resistance retrotransposition assays. HeLa cells were transfected with 1000 ng of CMV-L1-neo^{RT}, MusD-neo^{TNF}, IAP-neo^{TNF} or pcDNA3.1 DNA with 250, 500, and 1000 ng SLFN5 DNA, respectively, and then performed a retrotransposition assay (left panel). SLFN5 expression was monitored by Western blot using an anti-Flag probe (right panel). The colony numbers represent LINE-1 retrotransposition activity. Colonies were visualized with crystal violet staining. The data from three independent experiments are summarized in the bar graph.

LINE-1, resulting in almost no visible colonies (Figure 2B). Since IAP is the most active and mutagenic LTR retrotransposon in mice, it is tempting to speculate that mouse SLFN5 might possess the ability to regulate IAP retrotransposition. Thus, we also cloned mouse SLFN5 into the pcDNA4.0 vector, and test its regulation on IAP retrotransposition. As expected, we observed a significant inhibition of IAP by mouse SLFN5 which indicates the function of SLFN5 in controlling the mobilization of IAP is evolutionally conserved (Figure S2). While the mechanism underlying the selective effect of SLFN5 is under defined, the data suggest that SLFN5 possesses the inhibitory activity against some of LTR retrotransposons in addition to non-LTR LINE-1.

Helicase motifs are involved in the anti-LINE-1 activity of SLFN5

To explore the mechanism underlying the anti-LINE-1 activity of SLFN5, we first attempted to identify the involved motifs within SLFN5. A series of SLFN5 deletion mutants with Myc tags were constructed as shown in Figure 3A (upper panel). HeLa cells were cotransfected with CMV-L1-neo^{RT} DNA and wild-type or mutant SLFN5 constructs, and then, the cells were collected for immunoblotting assays and retrotransposition assays. The results showed that all SLFN5 deletion mutants are impaired in their ability to restrict LINE-1 retrotransposition. We noticed that while the N-terminal deletion mutants, which include the 1–450 aa sequence of SLFN5, still retained some LINE-1 restricting activity, all three C-terminal mutants, including the 335–891 aa sequence, completely lost their activity (Figure 3A, bottom panel), suggesting an essential prerequisite of SLFN5 C-terminus for its LINE-1 restricting activity.

Of note, SLFN5 contains a DNA/RNA helicase-like structure in its C-terminus, which was reported to process ATP-dependent DNA or RNA structure remodeling activity.[40] It is therefore interesting to know if the helicase motif of SLFN5 contributes to suppress LINE-1 retrotransposition. Most helicases consist of characteristic motifs (I, Ia, Ib, II, III, IV, V, and VI). Motifs I and II (Walker A and B motifs) are highly conserved and are essential for ATP binding and ATP hydrolysis activity respectively.[50] The Walker A and B consensus sequences consists of GxxxxGK(T/S) (where x is any amino acid) and hhhhD(D/E) (where h is a hydrophobic amino acid). Point mutations were thus introduced in the Walker A and B motifs (positions 584 and 649) of SLFN5 by substituting Lys^{584} and Asp^{649} with Arg and Ala, respectively (Figure 3A, upper panel). The results of the retrotransposition assay showed that the mutants SLFN5 (D649A) and SLFN5 (K584R/D649A) had almost completely lost all inhibitory activity against LINE-1, whereas SLFN5 (K584R) maintained most of its anti-LINE-1 activity compared to wild-type SLFN5 (Figure 3B). This result suggests that the helicase-like structure of SLFN5, especially the Walker B motif, is involved in the LINE-1 inhibition of SLFN5, which may confer to the function of SLFN5 C-terminus mentioned above.

SLFN5 reduces the copy numbers of LINE-1 DNA

The observation that SLFN5 inhibited LINE-1 transposition suggests reduced copy numbers of LINE-1 DNA in the presence of SLFN5. To test this hypothesis, we measured the LINE-1 DNA level in the presence or absence of SLFN5 by qPCR. To eliminate false signals from transfected CMV-L1-neo^{RT} reporter plasmid DNA, we employed a pair of primers, in which the forward primer was designed to solely anneal to the spliced neomycin resistance gene, such that only the LINE-1 DNA that has been reverse transcribed from the spliced RNA can be amplified (Figure 4A, upper panel). The results showed that SLFN5 expression decreased the LINE-1 DNA level in a dose-dependent manner (Figure 4A, lower left panel), consistent with the retrotransposition assay results. In contrast to wild-type SLFN5, all the mutants containing D649A, which lost the ability to inhibit LINE-1, exhibited no effects on LINE-1 DNA levels (Figure 4A, lower right panel). The results demonstrate that SLFN5 can decrease the LINE-1 DNA level, which includes the copy numbers of LINE-1 DNA and single-strand cDNA synthesized during the TPRT step.

To identify whether SLFN5 can decrease the LINE-1 single-stranded cDNA level, we analyzed the single-stranded cDNA level in the DNA-RNA hybrids using DRIP-qPCR. Briefly, the RNA-DNA hybrid was immunoprecipitated by the S9.6 antibody that specifically recognizes the RNA/DNA heteroduplex conformation, followed by quantification of LINE-1 DNA in the hybrid. The relative amount of cDNA in the DNA-RNA hybrid immunoprecipitates is represented as the fold change over the input level of LINE-1 cDNA. The data showed that SLFN5 reduced LINE-1 cDNA levels in DNA-RNA hybrids immunoprecipitated by S9.6 antibody by ~50% (Figure 4B), indicating that SLFN5 decreased the single-strand LINE-1 cDNA level during the retrotransposition process.

Since SLFN5 decreased LINE-1 cDNA levels, it is plausible that SLFN5 might affect the reverse transcription process, termed TPRT, catalyzed by RT activity of the LINE-1 ORF2p protein. We analyzed the influence of SLFN5 on the RT activity of LINE-1 using an *in vitro* LEAP assay. This assay was designed to synthesize LINE-1 cDNA from isolated LINE-1 RNP by mimicking the initial stages of TPRT, and the RT activity of LINE-1 RNP can be detected by quantifying the synthesized LINE-1 cDNA level. Using equal amounts of RNPs isolated from cells transfected CMV-L1-neo^{RT} with SLFN5 or control plasmids, we analyzed LINE-1 single-strand cDNA products in LEAP reactions containing isolated RNPs from each sample following the LEAP protocol of Kulpa and Moran.[3,51] The results showed a similar level of LEAP products regardless of the overexpression of SLFN5 (Figure 4C), suggesting that SLFN5 did not affect the TPRT process of LINE-1. Additionally, we also investigate the

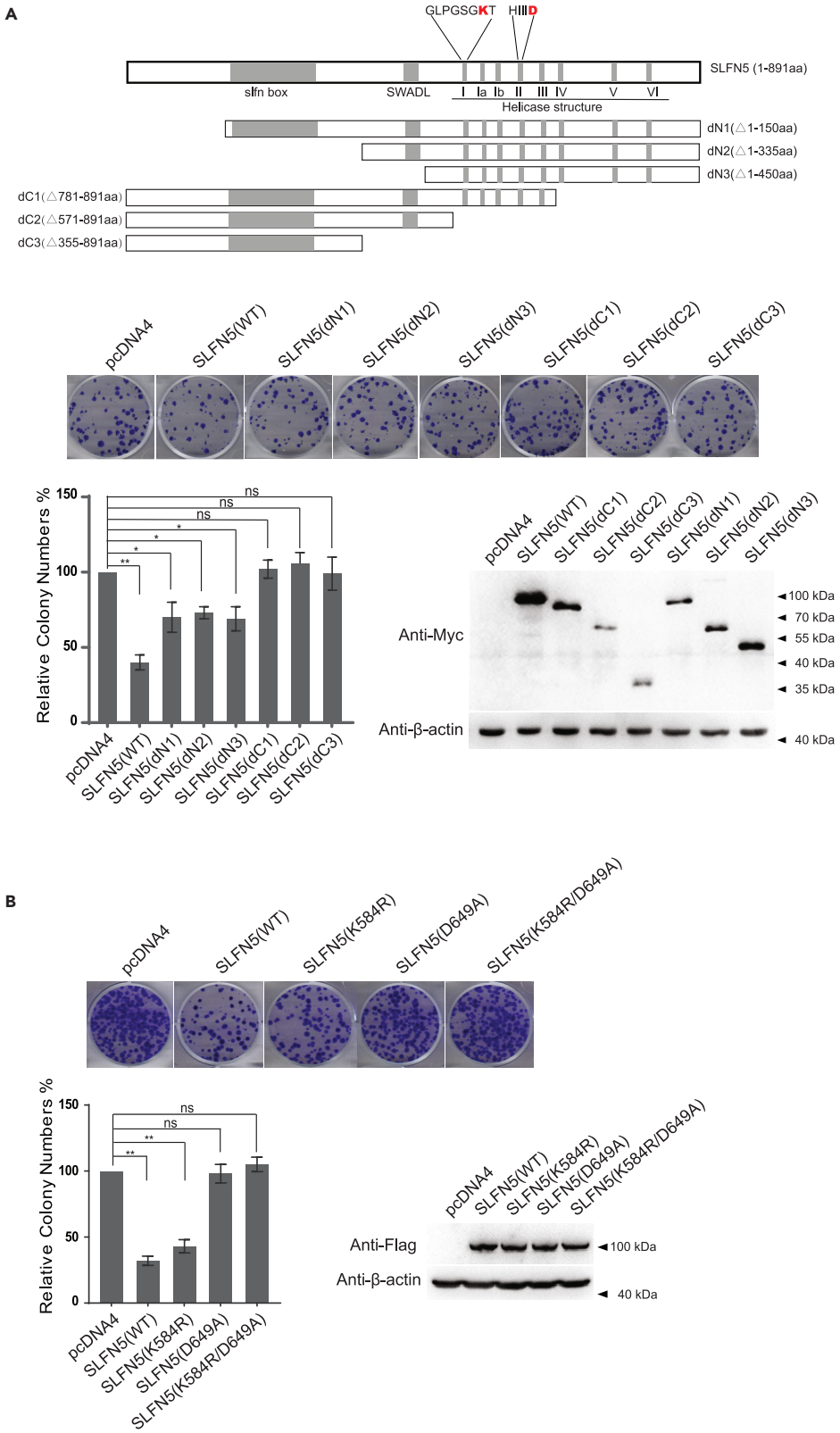
A
GLPGSGKT
HIIID
SLFN5 (1-891aa)
slfn box
SWADL
I Ia Ib II III IV V VI
Helicase structure
dN1(△1-150aa)
dN2(△1-335aa)
dN3(△1-450aa)
dC1(△781-891aa)
dC2(△571-891aa)
dC3(△355-891aa)
pcDNA4
SLFN5(WT)
SLFN5(dN1)
SLFN5(dN2)
SLFN5(dN3)
SLFN5(dC1)
SLFN5(dC2)
SLFN5(dC3)
Relative Colony Numbers %
150
100
50
0
ns
ns
ns
*
*
**
pcDNA4
SLFN5(WT)
SLFN5(dN1)
SLFN5(dN2)
SLFN5(dN3)
SLFN5(dC1)
SLFN5(dC2)
SLFN5(dC3)
Anti-Myc
Anti-β-actin
100 kDa
70 kDa
55 kDa
40 kDa
35 kDa
40 kDa
B
pcDNA4
SLFN5(WT)
SLFN5(K584R)
SLFN5(D649A)
SLFN5(K584R/D649A)
Relative Colony Numbers %
150
100
50
0
ns
ns
**
**
pcDNA4
SLFN5(WT)
SLFN5(K584R)
SLFN5(D649A)
SLFN5(K584R/D649A)
Anti-Flag
Anti-β-actin
100 kDa
40 kDa

Figure 3. Helicase motifs are required for SLFN5 to inhibit LINE-1 retrotransposition

(A) Upper panel: Scheme of the domain architecture of the wild-type and mutant SLFN5 variants tested. The numbers indicate the amino acid deletions in SLFN5 mutants. The positions of the mutated amino acids Lys and Asp in the Walker A and Walker B motifs are also indicated. Lower panel: The inhibitory activity of SLFN5 and its mutants. HeLa cells were transfected with CMV-L1-neo^{RT} DNA and SLFN5 or SLFN5 mutant plasmids, respectively, followed by retrotransposition assays. SLFN5 and its mutant expression were monitored by Western blotting using an anti-Flag probe. The colony numbers represent LINE-1 mobilization activity. Colonies were visualized with crystal violet staining. The data from three independent experiments are summarized in the bar graph.

(B) Detection of the inhibitory activity of SLFN5, SLFN5 (K584R), SLFN5 (D649A) and SLFN5 (K584R/D649A) on LINE-1 using a retrotransposition assay. The data from three independent experiments are summarized in the bar graph. Throughout the figure, statistical significance was determined by unpaired two-tailed Student's t test. n.s. not significant, *$p < 0.05$, **$p < 0.01$.

impact of SLFN5 on both exogenous and endogenous ORF2p localization by confocal microscope. Ectopic ORF2p transfected into HeLa cells and endogenous ORF2p in HeLa cells are both mainly located in the nucleus, irrespective of SLFN5 overexpression (Figure S3).

SLFN5 did not affect LINE-1 RNA transcription and translation

Before the TPRT process, LINE-1 RNA was first transcribed and served as mRNA for protein expression and RNA template to produce new cDNA copies. LINE-1 RNA levels affected the copy numbers of LINE-1 DNA. We therefore next examined the effect of SLFN5 on LINE-1 RNA levels, as determined by RT–qPCR. The results showed that different doses of ectopic SLFN5 expression did not significantly affect the LINE-1 RNA level (Figure 5A). To further assess the impact of SLFN5 knockout on endogenous L1 expression, the LINE-1 RNA levels in SLFN5-KO-HeLa cells and Ctrl-HeLa cells were evaluated. No remarkable increase in LINE-1 RNA was observed in SLFN5-KO-HeLa cells when compared to control group (Figure 5B, right panel). Moreover, a similar level of LINE-1 RNA was found in both CMV-L1-neo^{RT}-transfected SLFN5 knockout cells and control clones (Figure 5B, left panel). These results indicated that the SLFN5 level had no impact on the amount of LINE-1 RNA. In agreement with this finding, we observed that SLFN5 had no obvious effect on LINE-1 promoter activity (Figure 5C) using a report construct L1-FL,[33] which had the LINE-1 5′ UTR sequence inserted upstream of a firefly luciferase reporter gene in the pGL3 plasmid. Similar to the RNA data, we found that in HeLa cells cotransfected with LINE-1 and SLFN5 DNA, SLFN5 did not decrease LINE-1 ORF1p expression (Figure 5D), suggesting no effect of SLFN5 on LINE-1 protein expression. These data collectively demonstrate that SLFN5 has no obvious influence on LINE-1 at the transcriptional and translational levels.

SLFN5 decreased nuclear LINE-1 RNA level

Once LINE-1 RNA and proteins are expressed, the LINE-1 RNA associated with ORF1p and ORF2p in the form of RNP is imported into the nucleus where TPRT occurs.[52] Since SLFN5 diminished the LINE-1 cDNA level but did not affect its RNA level and RT activity, it is tempting to speculate that SLFN5 might influence LINE-1 RNA entry into the cell nucleus, consequently reducing the RNA template needed for LINE-1 cDNA synthesis. To test this hypothesis, we cotransfected 293T cells with CMV-L1-neo^{RT} plasmid and different amounts of SLFN5 DNA, isolated the nucleus and quantified the LINE-1 RNA level. The results clearly revealed that the ectopic expression of SLFN5 diminished the LINE-1 mRNA level in the nucleus, and the reduction in the nuclear content of LINE-1 mRNA was directly correlated with the SLFN5 expression level (Figure 6A).

We also compared the effect of wild-type and mutant SLFN5 on the nuclear entry of LINE-1 RNA. The results showed that both SLFN5 and active mutant SLFN5 (K584R) significantly diminished the amount of LINE-1 mRNA in the nucleus (Figure 6B), accompanied by a moderate increase in LINE-1 RNA levels in the cytoplasm (Figure 6C). In contrast, the inactive mutants SLFN5 (D649A) and SLFN5 (K584R/D649A) did not change the subcellular distribution of LINE-1 RNA (Figures 6B and 6C). In addition, we found that with the decrease in RNA in the nucleus, the ectopic expression of SLFN5 also diminished the ORF1p levels in a dose-dependent manner in the nucleus (Figure 6D), which is the key component of LINE-1 RNP. These data suggested that SLFN5 inhibits the nuclear entry of LINE-1 RNP rather than RNA alone. This observation is further supported by the RNA fluorescence in situ hybridization (FISH) assay data. The results showed that without SLFN5 expression, LINE-1 RNA was mainly concentrated in the nuclear region, while in the presence of SLFN5, LINE-1 RNA was spread throughout the cell, including the nucleus and cytoplasm (Figure 6E), indicating a decreasing ratio of LINE-1 mRNA levels in the nuclear region. Furthermore, the image also showed a co-localization of SLFN5 and LINE-1 RNA, thus indicating an interaction between SLFN5 and LINE-1 RNA or RNP.

SLFN5 interrupted the formation of LINE-1 RNP

Because the formation of LINE-1 RNP is a prerequisite for nuclear entry of LINE-1 RNA, the inefficient importation of LINE-1 RNP into the nucleus may result from either failure of RNP formation or the subsequent import process. To examine this problem, we first determined whether SLFN5 influenced the formation of LINE-1 RNP, as determined by quantification of RNP in ultracentrifugation pellets using an Odyssey infrared imaging system. Compared to the inactive mutants SLFN5 (D649A) and SLFN5 (K584R/D649A), the presence of SLFN5 reduced the ratio of ORF1p in the RNP to total cell lysis (Figure 7A), suggesting that SLFN5 may influence the formation of LINE-1 RNP. We next examined the level of LINE-1 RNA binding to ORF1p in the presence of SLFN5 or its mutants using an RIP assay. The results showed that, comparing the inactive SLFN5 mutants D649A and K584R/D649A, SLFN5 greatly diminished the LINE-1 RNA level binding to ORF1p, indicating an impaired interaction between LINE-1 RNA and ORF1p, which serves as a hallmark of LINE-1 RNP formation, confirming that SLFN5 can interfere with the formation of LINE-1 RNP (Figure 7B). To further verify this result, we cotransfected 293T cells with the CMV-L1-neo^{RT} plasmid and

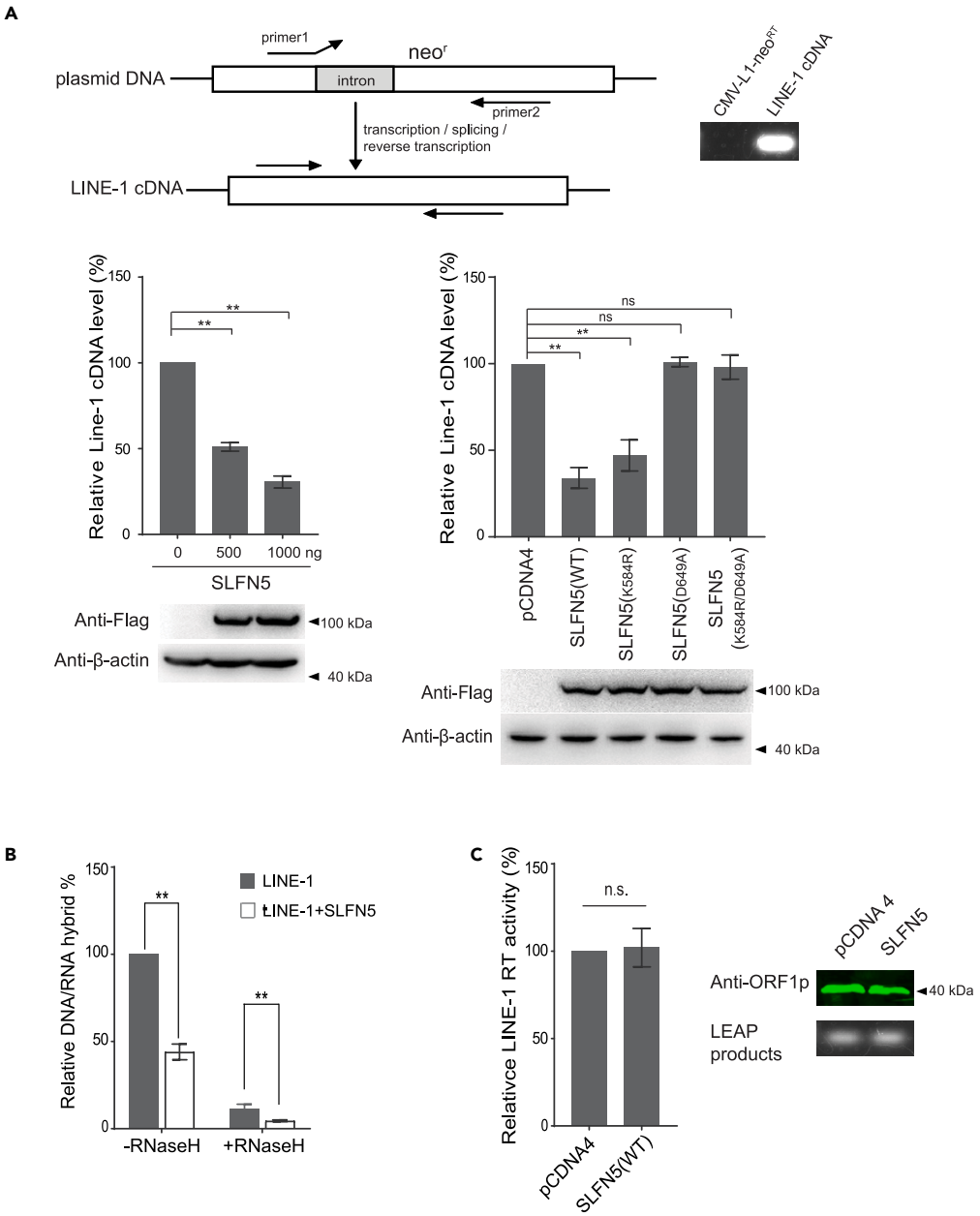

Figure 4. SLFN5 diminished LINE-1 cDNA levels but did not affect its reverse transcriptase activity

(A) SLFN5 can diminish LINE-1 cDNA. Upper panel(left): Illustration of the primer locations used for amplifying CMV-L1-neo^{RT} cDNA. Upper panel (right): PCR products of the plasmid DNA and reverse transcribed cDNA of CMV-L1-neo^{RT} by the designed primers. The lower panel (left): HeLa cells were cotransfected with 1000 ng CMV-L1-neo^{RT} DNA with 0, 500 and 1000 ng SLFN5-expressing plasmids, and then LINE-1 cDNA was detected by qPCR. The lower panel (right): HeLa cells were cotransfected with 1000 ng CMV-L1-neo^{RT} DNA with 500 ng SLFN5, SLFN5 (K584R), SLFN5 (D649A) and SLFN5 (K584R/D649A) DNA, and then LINE-1 cDNA was detected by qPCR. The data from three independent experiments are summarized in the bar graph. The expression of SLFN5 was detected by Western blot.

(B) DRIP-qPCR was performed in SLFN5-transfected HeLa cells and control cells. The relative abundance of the DNA-RNA hybrid is represented as the fold change over the control. The sample with RNase H treatment was set as a negative control, in which the RNA strands of the RNA-DNA hybrids were specifically removed and therefore could not be immunoprecipitated by the S9.6 antibody.

(C) SLFN5 did not affect the reverse transcriptase activity of LINE-1 ORF2p. HeLa cells were transfected with 1000 ng CMV-L1-neo^{RT} DNA with 500 ng SLFN5, and 48 h later, the cells were collected to detect reverse transcriptase activity by LEAP assay. The reverse transcribed cDNA was quantified by qPCR (left panel) and visualized by conventional PCR (bottom right panel), and the data from three independent experiments are summarized in the bar graph. Throughout the figure, statistical significance was determined by unpaired two-tailed Student's *t* test. *$p < 0.05$; **$p < 0.01$; n.s., not significant.

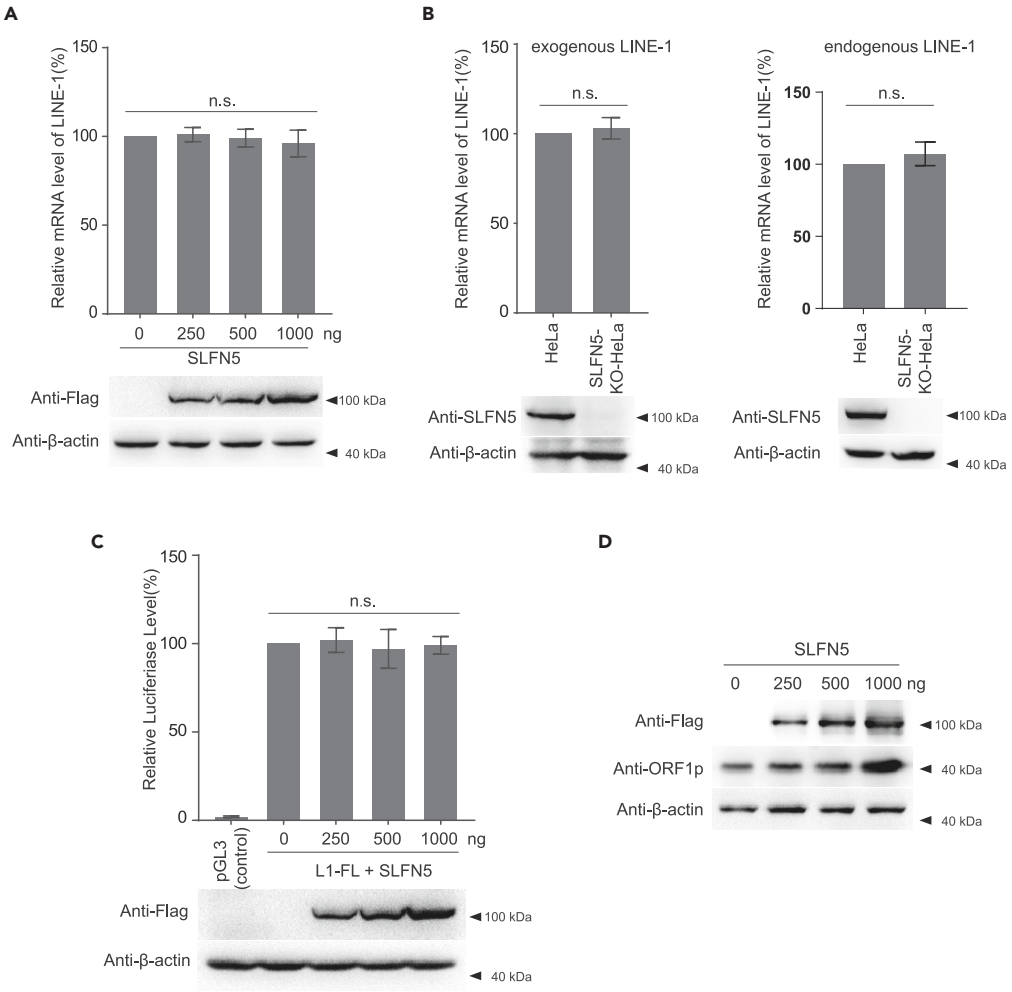

Figure 5. SLFN5 has no effect on the transcription and translation of LINE-1

(A) Exogenous expressing SLFN5 did not decrease LINE-1 RNA level. HeLa cells were transfected 1000 ng CMV-L1-neo^{RT} DNA with 250, 500 and 1000 ng of SLFN5 plasmids respectively. 48 h later, the cells were collected for total RNA extraction, and performed RT-qPCR.

(B) SLFN5 knockout did not affect LINE-1 RNA level. SLFN5-KO-HeLa cell line, and control HeLa cell line were transfected with 1000 ng CMV-L1-neo^{RT} DNA, and then total cellular RNA was extracted for RT–qPCR (left panel). 1x10^{6} of SLFN5-KO-HeLa cells and control cells were harvested and total RNA was extracted to detect endogenous LINE-1 RNA expression by RT–qPCR (right panel). SLFN5 expression was monitored by Western blot using an anti-Flag probe. The RT–qPCR data from three independent experiments are summarized in the bar graph.

(C) SLFN5 did not inhibit the 5′UTR promoter activity of LINE-1. HEK293 cells were cotransfected with 1000 ng L1-FL DNA together with 250, 500 and 1000 ng of SLFN5 plasmids. The firefly luciferase activity was measured to represent the activity of the LINE-1 5′-UTR promoter. pGL3-basic contains the firefly luciferase gene that lacks a promoter at its 5′ end. Firefly luciferase activity from this vector was measured to reflect the basal expression of the firefly luciferase gene. SLFN5 expression was monitored by Western blot using an anti-Flag probe. The luciferase activity assay from three independent experiments is summarized in the bar graph.

(D) SLFN5 expression did not affect LINE-1 RNA translation. HeLa cells were transfected with CMV-L1-neo^{RT} DNA with 250, 500 and 1000 ng of SLFN5 plasmids. The cell lysates were used to detect SLFN5 (anti-Flag), ORF1p (anti-ORF1p) and β-actin (anti-β-actin) expression using Western blotting. Throughout the figure, statistical significance was determined by unpaired two-tailed Student's *t* test. n.s., not significant.

SLFN5 DNA or its mutant SLFN5 (K584R/D649A) and then collected cell lysates for subcellular fractionation analysis. Extracts of such cells were separated into a 5%–50% discontinuous sucrose gradient by ultracentrifugation, and the distribution of LINE-1 RNA and ORF1p protein levels was examined by RT–qPCR and Western blot, respectively (Figure 7C). In the cells transfected with pcDNA4 or mutant SLFN5(K584R/D649A), almost all LINE-1 RNA and ORF1p protein were present in high-density sucrose gradients, indicating that they existed in the form of RNP complex, which possess high molecular weight. In the cells transfected with wild-type SLFN5, a large proportion of LINE-1 RNA and ORF1p protein shifted to low-density sucrose gradients, which suggested a low molecular weight-free form. Taken together, these data support an inhibitory effect of SLFN5 on RNP formation, which contributes to reduced nuclear LINE-1 RNA level.

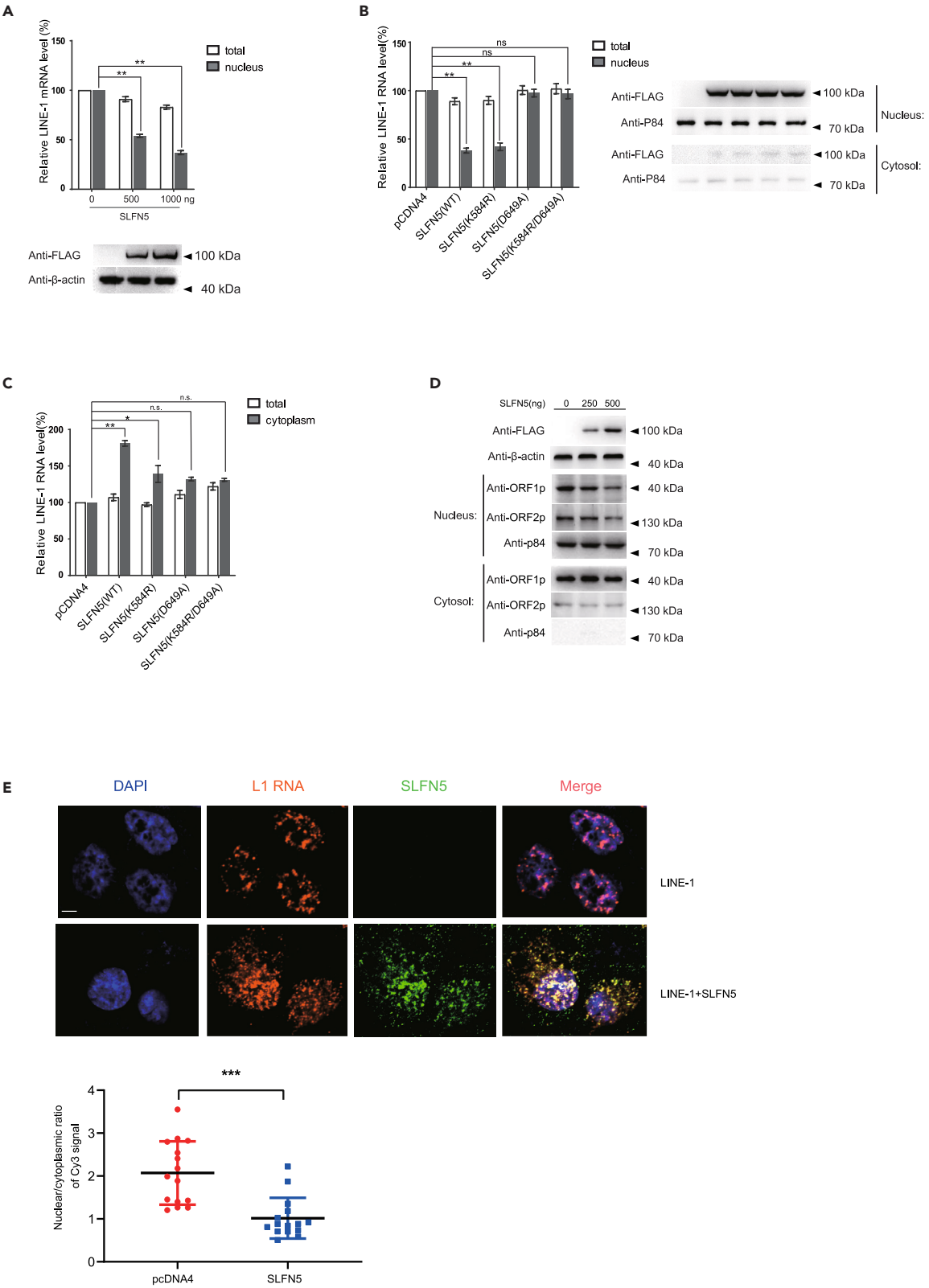
A
Relative LINE-1 mRNA level (%)
total
nucleus
0
500
1000 ng
SLFN5
Anti-FLAG
Anti-β-actin
100 kDa
40 kDa
B
Relative LINE-1 RNA level(%)
ns
total
nucleus
Anti-FLAG
Anti-P84
100 kDa
70 kDa
Nucleus:
Cytosol:
pCDNA4
SLFN5(WT)
SLFN5(K584R)
SLFN5(D649A)
SLFN5(K584R/D649A)
C
Relative LINE-1 RNA level(%)
n.s.
total
cytoplasm
D
SLFN5(ng)
0 250 500
Anti-FLAG
Anti-β-actin
Anti-ORF1p
Anti-ORF2p
Anti-p84
40 kDa
130 kDa
70 kDa
Nucleus:
Cytosol:
E
DAPI
L1 RNA
SLFN5
Merge
LINE-1
LINE-1+SLFN5
***
Nuclear/cytoplasmic ratio of Cy3 signal
pcDNA4
SLFN5

Figure 6. SLFN5 decreased nuclear LINE-1 RNA level

(A) SLFN5 blocks LINE-1 RNA entering nucleus. HeLa cells were cotransfected with CMV-L1-neo^{RT} and different amounts of SLFN5 DNA. Forty-eight hours later, cells were collected for extracting whole cell and nuclear RNA to quantify the LINE-1 RNA level by RT–qPCR. The expression of SLFN5 was detected by Western blot.

(B) The effects of SLFN5 and its mutants on LINE-1 RNA levels in the nucleus (left panel). The expression of SLFN5 was detected by Western blot. p84 protein and β-actin was used as a nuclear and cytoplasmic marker (right panel).

(C) The effects of SLFN5 and its mutants on LINE-1 RNA levels in the cytoplasm.

(D) Detection of the effects of SLFN5 on the ORF1p and ORF2p levels in the nucleus and cytoplasm by Western blot. p84 protein and β-actin was used as a nuclear and cytoplasmic marker.

(E) SLFN5 changed the distribution of LINE-1 RNA in cells. Upper panel: Confocal microscopy showed subcellular localization of LINE-1 RNA (red) and SLFN5 (green). Lower panel: Quantification of subcellular localization of LINE-1 RNA was performed on 15 individual cells for each sample by measuring the fluorescence intensities of nuclear and cytoplasmic subcompartments per cell. The scale bar represents 10 μm. The data from three independent experiments are summarized in the bar graph. Throughout the figure, statistical significance was determined by unpaired two-tailed Student's *t* test. *$p < 0.05$; **$p < 0.01$. n.s., not significant.

From Figure 7C, we also noticed that both WT SLFN5 or SLFN5 (K584R/D649A) appeared in the same gradient with that of LINE-1 RNA, no matter in the high or low molecular weight form, suggesting that SLFN5 might directly associate with LINE-1 RNA instead of ORF1p. Indeed, we failed to find any interaction between SLFN5 and LINE-1 ORF1p (Figure S4A), but detected the association between SLFN5 and LINE-1 RNA (Figure S4B). Notably, enzymatic-inactive mutants of SLFN5 retained the interaction with LINE-1 RNA. We next tested a variety of SLFN5 deletion mutants and the data showed that there were no obvious changes in the association of SLFN5 with LINE-1 RNA by removing the N-terminal 1–150 aa sequences and C-terminal motifs (335–891 aa). However, the N-terminal 151–355 aa deletion, which contains a slfn box domain, greatly impaired the interaction of SLFN5 with LINE-1 RNA. A larger N-terminal SLFN5 deletion dN3 (Δ1-450 aa) also impaired its interaction with LINE-1 RNA (Figure 7D). These data suggest that the N-terminal domain of SLFN5, especially the 151–335 aa sequence, is required for the interaction between SLFN5 and LINE-1 RNA. The slight increase in the binding activity found in C-terminal deletion mutants might reflect an altered conformation affecting the neighboring RNA-binding site in SLFN5. Furthermore, to exclude the possibility that SLFN5 binds LINE-1 RNA in a non-specific manner, we also determined whether SLFN5 was able to bind to GAPDH, MDM2 and actin RNA. None of these RNAs were enriched by SLFN5 compared with the IgG group (Figure S4C). Collectively, these results suggested a mechanism that SLFN5 impair the formation of LINE-1 RNP might by directly binding to LINE-1 RNA and dissociation of ORF1p through its helicase activity.

DISCUSSION

In this study, we provided evidence showing that IFN-inducible SLFN5 serves as a potent restriction factor of LINE-1 transposition. Further mechanistic studies revealed that SLFN5 inhibited the formation of LINE-1 RNP and its subsequent nuclear entry, thus diminishing the RNA template used for LINE-1 cDNA production. This highlights a new mechanism for the host to negatively control the transposition of LINE-1, together with the means from other host factors reported previously,[21,26,28,33,34,53–55] providing multilayer protection to maintain genetic stability.

LINE-1 RNP particles are a large complex comprising ORF1p trimers, ORF2p and LINE-1 RNA, and their assembly is mainly mediated by the interaction between the structural protein ORF1p and the RNA. There is an ongoing debate over whether LINE-1 RNPs is imported into nucleus through nuclear pore passively[56–59] or mediated by cell cycle during which nuclear membrane breaks down, allowing the possible entrance of LINE-1 RNPs into the nucleus.[60–62] Nevertheless, the formation of LINE-1 RNP and the accessibility of RNP to nuclear DNA is necessary for LINE-1 retrotransposition despite the way RNPs exploit for its nuclear entry. We failed to detect the binding of SLFN5 to ORF1p (Figure S4A), which preliminarily excluded the possibility that SLFN5 blocked the interaction between LINE-1 ORF1p and RNA by binding to ORF1p. Instead, both RNA FISH analysis and RIP experiments revealed that SLFN5 exhibited a potent ability to interact with LINE-1 RNA, and aa 151–335 in the N-terminal domain is essential for this interaction. However, it should be noted that the binding of SLFN5 to LINE-1 RNA is insufficient for blocking the association between LINE-1 RNA and ORF1p, since the SLFN5 mutants unable to inhibit LINE-1 were found to interact with LINE-1 RNA (Figure 3B). Of note, SLFN5 possesses a DNA/RNA helicase-like structure, and we found that any deletion that affects the integrity of the helicase domain or even a single amino acid mutation in the conserved motif of the structure will cause SLFN5 to lose its inhibitory activity, suggesting an important role of this structure in anti-LINE-1 activity. Early studies have shown that RNA helicases are highly conserved enzymes that have ATP-dependent double-stranded RNA or RNA/DNA duplex unwinding activity. Recently, it was revealed that RNA helicases also have ATP-dependent RNA-protein complex remodeling activity, including removal of RNA-binding proteins from mRNA transcripts.[63] For example, MOV10, another RNA helicase, was able to promote target mRNP disassembly by removing proteins and/or resolving secondary structures.[31]

Therefore, it is plausible to speculate that SLFN5 may exert its inhibitory activity against LINE-1 by binding to LINE-1 RNA, and then dissociate or partially dissociate ORF1p from LINE-1 RNA through its helicase activity, resulting in impaired RNP formation, which finally affects the nuclear entry of LINE-1 RNA. Additionally, we noticed a failure of dN1 to restore the inhibitory function of full-length SLFN5 indicates SLFN5$^{1-150}$ is also required for its anti-LINE-1 activity, possibly due to its influence on the conformational rearrangement of SLFN5. Indeed, beneficial from the resolved SLFN5 cyro-EM structure by Katja Lammens' group,[64] it has been demonstrated that the N-terminal 144 residues of SLFN5 core domain forms a second large interface with the linker domain which is crucial for connecting C-terminal helicase with

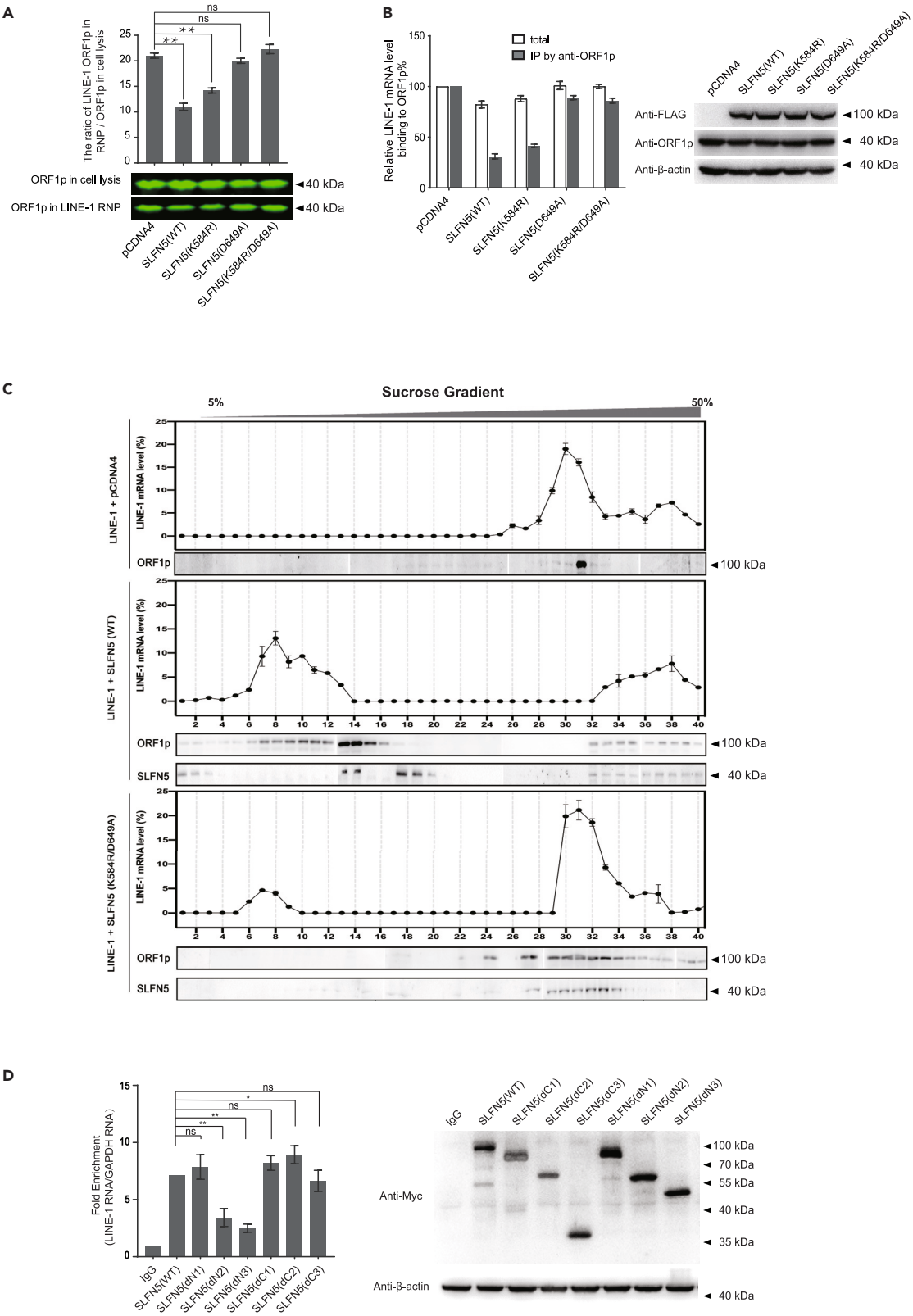
A
The ratio of LINE-1 ORF1p in RNP / ORF1p in cell lysis
ns
ns
**
**
ORF1p in cell lysis
ORF1p in LINE-1 RNP
◄40 kDa
◄40 kDa
pCDNA4
SLFN5(WT)
SLFN5(K584R)
SLFN5(D649A)
SLFN5(K584R/D649A)
B
Relative LINE-1 mRNA level binding to ORF1p%
total
IP by anti-ORF1p
Anti-FLAG
Anti-ORF1p
Anti-β-actin
◄100 kDa
◄ 40 kDa
◄ 40 kDa
C
Sucrose Gradient
5%
50%
LINE-1 + pCDNA4
LINE-1 + SLFN5 (WT)
LINE-1 + SLFN5 (K584R/D649A)
LINE-1 mRNA level (%)
ORF1p
SLFN5
◄100 kDa
◄ 40 kDa
D
Fold Enrichment (LINE-1 RNA/GAPDH RNA)
ns
*
**
**
ns
IgG
SLFN5(WT)
SLFN5(dN1)
SLFN5(dN2)
SLFN5(dN3)
SLFN5(dC1)
SLFN5(dC2)
SLFN5(dC3)
Anti-Myc
Anti-β-actin
◄100 kDa
◄ 70 kDa
◄ 55 kDa
◄ 40 kDa
◄ 35 kDa
◄ 40 kDa

Figure 7. SLFN5 binds to LINE-1 RNA and blocks the recruitment of ORF1p required for LINE-1 RNP

(A) SLFN5 affects the formation of LINE-1 RNP. HeLa cells were cotransfected with 1000 ng CMV-L1-neo^{RT} DNA and 500 ng SLFN5, SLFN5 (K584R), SLFN5 (D649A) or SLFN5 (K584R/D649A) DNA. Forty-eight hours later, equal amounts of cell lysates were used to isolate LINE-1 RNP by ultracentrifugation. The LINE-1 RNP samples were quantified by detecting LINE-1 ORF1p using the Odyssey infrared imaging system.

(B) SLFN5 and its mutants bind to LINE-1 RNA. HeLa cells were cotransfected with CMV-L1-neo^{RT} DNA and SLFN5, SLFN5 (K584R), SLFN5 (D649A) and SLFN5 (K584R/D649A) DNA. Forty-eight hours later, an equal amount of cell lysis was used to detect LINE-1 RNA and SLFN5 by RNA IP. LINE-1 RNA pulled down by ORF1p was quantified by RT–qPCR. The expression of SLFN5 and ORF1p was detected by Western blot using anti-Flag and anti-ORF1p antibodies, respectively.

(C) The distribution of LINE-1 RNA and ORF1p was analyzed by 5%–50% discontinuous sucrose gradient ultracentrifugation. Each fraction collected was analyzed by RT–PCR and Western blot. The numbers under the graph represent different fractions.

(D) Detection of the interaction between LINE-1 RNA and SLFN5 mutants by RIP. Equal amounts of cell lysates were immunoprecipitated with anti-Myc, and the levels of LINE-1 and GAPDH RNA were determined by qRT–PCR. IgG served as the negative control in the RIP. The data from three independent experiments are summarized in the bar graph. The expression of SLFN5 and its mutants was detected by Western blot. Throughout the figure, statistical significance was determined by unpaired two-tailed Student's *t* test. *$p < 0.05$; **$p < 0.01$; ns, not significant.

N-terminal core domain. It can be speculated that N-terminal residues might play a key role in stabilizing the structural arrangement of SLFN5, thus reinforcing the C-terminal helicase activity.

Our evidence presented herein supports that SLFN5 interrupts LINE-1 RNP formation in the cytoplasm, while it is worth noting that SLFN5 has been presumed to be a nuclear protein in previous studies.[65] Interestingly, we found relocalization of partial SLFN5 from the nuclei into the cytoplasmic foci when stimulated by IFN (Figure S1E). Similarly, obvious cytoplasmic localization of SLFN5 was found upon coexpression of LINE-1 (Figure 6E). These observations suggest that SLFN5 might relocate to the cytoplasm in response to certain stresses, such as LINE-1 and IFN, allowing it to exert functions in the cytoplasm. The corresponding nuclear export signals in SLFN5 amino acid sequences merit further investigations.

Moreover, our studies showed that SLFN5 also potently inhibited IAP, suggesting its relatively broad activity against different species of retrotransposons. It is interesting that IAP and MusD, which share a similar genetic configuration, display a distinct vulnerability to SLFN5 inhibition, possibly due to LTR nucleotide variability between these two murine LTR retrotransposons, while the detailed mechanism underlying the anti-IAP activity of SLFN5 awaits further investigation.

LINE-1 RNA and protein overexpression is a hallmark of human cancers. A wide variety of tumor cell lines and tissues, such as renal, ovarian, lung carcinomas and melanoma, express LINE-1 RNA and/or protein at detectable levels.[66–69] Meanwhile, restricting LINE-1 by siRNA or RT inhibitors was reported to promote senescence and differentiation and reduce the invasive growth of cancer cells.[70–73] These clues suggested that LINE-1 might drive directly or contribute indirectly to tumorigenesis. Being derived (or evolved) from ancient retroviruses, LINE-1 replicates through reverse transcription. During this process, LINE-1 might activate endogenous DNA and RNA sensors, triggering innate immune activation to promote interferon (IFN) expression.[74] The mobilization of LINE-1 leads to genomic instability and an increased propensity for tumor occurrence. SLFN5 is highly sensitive to IFN stimulation among Schlafen family members. Considering several lines of evidence indicating that SLFN5 has potent antitumor activity against melanoma[44] and RCC,[47] the antitumor activity of SLFN5 might be related to its inhibitory activity against LINE-1 transposition as an ISG, which warrants further investigation.

Limitations of the study

There are several limitations to our study that should be acknowledged. First, the mechanism by which SLFN5 disrupts LINE-1 RNP formation remains unclear. It is unknown whether SLFN5 binding to LINE-1 RNA induces an inferior secondary structure that prevents ORF1p recruitment, or if SLFN5 competitively binds to LINE-1 RNA with ORF1p. Follow-up studies are required to mechanistically study how SLFN5 interferes with RNP formation. Second, despite conducting RNA-IP experiments with different SLFN5 mutants to analyze the structure-function relationship of SLFN5, we still cannot fully explain why dN1 is unable to restore the function of full-length SLFN5. It will be of interest to determine whether the N-terminal residues contribute to the anti-LINE-1 activity by stabilizing the structural arrangement. Lastly, due to the lack of suitable cell or animal models, we were unable to investigate whether the antitumor activity or interferon-regulating capacity of SLFN5 is related to its inhibitory activity against LINE-1 transposition.

STAR★METHODS

Detailed methods are provided in the online version of this paper and include the following:

- KEY RESOURCES TABLE
- RESOURCE AVAILABILITY
  - Lead contact
  - Materials availability
  - Data and code availability
- EXPERIMENTAL MODEL AND STUDY PARTICIPANT DETAILS
  - Cell lines
- METHOD DETAILS
  - Plasmids and antibodies

- Retrotransposition assay
- Quantification of LINE-1 RNA by RT–qPCR
- Quantification of reverse transcribed LINE-1 DNA by qPCR
- Cell nuclear and cytoplasmic extraction
- Western blotting
- LINE-1 element amplification protocol (LEAP)
- Co-Immunoprecipitation (CoIP) assay
- RNA immunoprecipitation (RIP)
- RNA fluorescence *in situ* hybridization (FISH)
- RNA-DNA hybrid immunoprecipitation (DRIP)
- Discontinuous sucrose gradient ultracentrifugation

● QUANTIFICATION AND STATISTICAL ANALYSIS

SUPPLEMENTAL INFORMATION

Supplemental information can be found online at https://doi.org/10.1016/j.isci.2023.107968.

ACKNOWLEDGMENTS

The authors wish to thank Thierry Heidmann for the gift CMV-L1-neo^{RT} reporter plasmid and Dr Haig H. Kazazian Jr and John L. Goodier for the SVA-neo and Alu-neo plasmids. We also thank Dr. Fei Guo for providing The ORF1p antibody (rabbit). This work was supported by the National Natural Science Foundation of China Grant 31870164; Chinese Academy of Medical Sciences innovation fund for Medical Sciences (CIFMS) 2021-I2M-1-043 to LXY and Chinese Scholarship Council (2022)1007 to DJW.

AUTHOR CONTRIBUTIONS

L.X. and C.S. conceived and supervised the project. J.D., S.W., and Q.L. carried out the bulk of the experimental work as well as data analysis. U.D., T.C.., Z.Y., A.Z., Q.L., and Z.Z. provided additional data and reagents. N.Z., Q.L., N.A., J.Z., D.Y., and Q.L. contributed to the data analysis. Z.C., J.W., and Y.Z. provided technical assistance with the sucrose gradient ultracentrifugation experiment. L.M. and S.G. helped with plasmid construction. J.D. and X.L. wrote the manuscript. L.C. J.Z., C.S., and J.W. helped with writing and proofreading the paper. All authors approved the final version of the manuscript.

DECLARATION OF INTERESTS

The authors declare no competing interests.

Received: November 18, 2022
Revised: July 20, 2023
Accepted: September 15, 2023
Published: September 19, 2023

REFERENCES

1. Brouha, B., Schustak, J., Badge, R.M., Lutz-Prigge, S., Farley, A.H., Moran, J.V., and Kazazian, H.H., Jr. (2003). Hot L1s account for the bulk of retrotransposition in the human population. Proc. Natl. Acad. Sci. USA *100*, 5280–5285. https://doi.org/10.1073/pnas.0831042100.
2. Babushok, D.V., and Kazazian, H.H., Jr. (2007). Progress in understanding the biology of the human mutagen LINE-1. Hum. Mutat. *28*, 527–539. https://doi.org/10.1002/humu.20486.
3. Kulpa, D.A., and Moran, J.V. (2006). Cis-preferential LINE-1 reverse transcriptase activity in ribonucleoprotein particles. Nat. Struct. Mol. Biol. *13*, 655–660. https://doi.org/10.1038/nsmb1107.
4. Luan, D.D., Korman, M.H., Jakubczak, J.L., and Eickbush, T.H. (1993). Reverse transcription of R2Bm RNA is primed by a nick at the chromosomal target site: a mechanism for non-LTR retrotransposition. Cell *72*, 595–605. https://doi.org/10.1016/0092-8674(93)90078-5.
5. Christensen, S.M., Bibillo, A., and Eickbush, T.H. (2005). Role of the Bombyx mori R2 element N-terminal domain in the target-primed reverse transcription (TPRT) reaction. Nucleic Acids Res. *33*, 6461–6468. https://doi.org/10.1093/nar/gki957.
6. Denli, A.M., Narvaiza, I., Kerman, B.E., Pena, M., Benner, C., Marchetto, M.C.N., Diedrich, J.K., Aslanian, A., Ma, J., Moresco, J.J., et al. (2015). Primate-specific ORF0 contributes to retrotransposon-mediated diversity. Cell *163*, 583–593. https://doi.org/10.1016/j.cell.2015.09.025.
7. Criscione, S.W., Theodosakis, N., Micevic, G., Cornish, T.C., Burns, K.H., Neretti, N., and Rodić, N. (2016). Genome-wide characterization of human L1 antisense promoter-driven transcripts. BMC Genom. *17*, 463. https://doi.org/10.1186/s12864-016-2800-5.
8. Kazazian, H.H., Jr., Wong, C., Youssoufian, H., Scott, A.F., Phillips, D.G., and Antonarakis, S.E. (1988). Haemophilia A resulting from de novo insertion of L1 sequences represents a novel mechanism for mutation in man. Nature *332*, 164–166. https://doi.org/10.1038/332164a0.
9. Miki, Y., Nishisho, I., Horii, A., Miyoshi, Y., Utsunomiya, J., Kinzler, K.W., Vogelstein, B., and Nakamura, Y. (1992). Disruption of the APC gene by a retrotransposal insertion of L1 sequence in a colon cancer. Cancer Res. *52*, 643–645.
10. Fodde, R., Smits, R., and Clevers, H. (2001). APC, signal transduction and genetic instability in colorectal cancer. Nat. Rev. Cancer *1*, 55–67. https://doi.org/10.1038/35094067.
11. Groden, J., Thliveris, A., Samowitz, W., Carlson, M., Gelbert, L., Albertsen, H., Joslyn, G., Stevens, J., Spirio, L., Robertson, M., et al. (1991). Identification and characterization of

the familial adenomatous polyposis coli gene. Cell *66*, 589–600.
12. Burns, K.H. (2017). Transposable elements in cancer. Nat. Rev. Cancer *17*, 415–424. https://doi.org/10.1038/nrc.2017.35.
13. Zamudio, N., and Bourc'his, D. (2010). Transposable elements in the mammalian germline: a comfortable niche or a deadly trap? Heredity *105*, 92–104. https://doi.org/10.1038/hdy.2010.53.
14. Swergold, G.D. (1990). Identification, characterization, and cell specificity of a human LINE-1 promoter. Mol. Cell Biol. *10*, 6718–6729.
15. Yoder, J.A., Walsh, C.P., and Bestor, T.H. (1997). Cytosine methylation and the ecology of intragenomic parasites. Trends Genet. *13*, 335–340.
16. Carmell, M.A., Girard, A., van de Kant, H.J.G., Bourc'his, D., Bestor, T.H., de Rooij, D.G., and Hannon, G.J. (2007). MIWI2 is essential for spermatogenesis and repression of transposons in the mouse male germline. Dev. Cell *12*, 503–514. https://doi.org/10.1016/j.devcel.2007.03.001.
17. Aravin, A.A., Hannon, G.J., and Brennecke, J. (2007). The Piwi-piRNA pathway provides an adaptive defense in the transposon arms race. Science *318*, 761–764. https://doi.org/10.1126/science.1146484.
18. Soifer, H.S., Zaragoza, A., Peyvan, M., Behlke, M.A., and Rossi, J.J. (2005). A potential role for RNA interference in controlling the activity of the human LINE-1 retrotransposon. Nucleic Acids Res. *33*, 846–856. https://doi.org/10.1093/nar/gki223.
19. Hamdorf, M., Idica, A., Zisoulis, D.G., Gamelin, L., Martin, C., Sanders, K.J., and Pedersen, I.M. (2015). miR-128 represses L1 retrotransposition by binding directly to L1 RNA. Nat. Struct. Mol. Biol. *22*, 824–831. https://doi.org/10.1038/nsmb.3090.
20. Yang, N., and Kazazian, H.H., Jr. (2006). L1 retrotransposition is suppressed by endogenously encoded small interfering RNAs in human cultured cells. Nat. Struct. Mol. Biol. *13*, 763–771. https://doi.org/10.1038/nsmb1141.
21. Kinomoto, M., Kanno, T., Shimura, M., Ishizaka, Y., Kojima, A., Kurata, T., Sata, T., and Tokunaga, K. (2007). All APOBEC3 family proteins differentially inhibit LINE-1 retrotransposition. Nucleic Acids Res. *35*, 2955–2964. https://doi.org/10.1093/nar/gkm181.
22. MacDuff, D.A., Demorest, Z.L., and Harris, R.S. (2009). AID can restrict L1 retrotransposition suggesting a dual role in innate and adaptive immunity. Nucleic Acids Res. *37*, 1854–1867. https://doi.org/10.1093/nar/gkp030.
23. Stenglein, M.D., and Harris, R.S. (2006). APOBEC3B and APOBEC3F inhibit L1 retrotransposition by a DNA deamination-independent mechanism. J. Biol. Chem. *281*, 16837–16841. https://doi.org/10.1074/jbc.M602367200.
24. Richardson, S.R., Narvaiza, I., Planegger, R.A., Weitzman, M.D., and Moran, J.V. (2014). APOBEC3A deaminates transiently exposed single-strand DNA during LINE-1 retrotransposition. Elife *3*, e02008. https://doi.org/10.7554/eLife.02008.
25. Chen, H., Lilley, C.E., Yu, Q., Lee, D.V., Chou, J., Narvaiza, I., Landau, N.R., and Weitzman, M.D. (2006). APOBEC3A is a potent inhibitor of adeno-associated virus and retrotransposons. Curr. Biol. *16*, 480–485. https://doi.org/10.1016/j.cub.2006.01.031.
26. Muckenfuss, H., Hamdorf, M., Held, U., Perković, M., Löwer, J., Cichutek, K., Flory, E., Schumann, G.G., and Münk, C. (2006). APOBEC3 proteins inhibit human LINE-1 retrotransposition. J. Biol. Chem. *281*, 22161–22172. https://doi.org/10.1074/jbc.M601716200.
27. Tan, L., Sarkis, P.T.N., Wang, T., Tian, C., and Yu, X.F. (2009). Sole copy of Z2-type human cytidine deaminase APOBEC3H has inhibitory activity against retrotransposons and HIV-1. FASEB J. *23*, 279–287. https://doi.org/10.1096/fj.07-088781.
28. Liang, W., Xu, J., Yuan, W., Song, X., Zhang, J., Wei, W., Yu, X.F., and Yang, Y. (2016). APOBEC3DE Inhibits LINE-1 Retrotransposition by Interacting with ORF1p and Influencing LINE Reverse Transcriptase Activity. PLoS One *11*, e0157220. https://doi.org/10.1371/journal.pone.0157220.
29. Arjan-Odedra, S., Swanson, C.M., Sherer, N.M., Wolinsky, S.M., and Malim, M.H. (2012). Endogenous MOV10 inhibits the retrotransposition of endogenous retroelements but not the replication of exogenous retroviruses. Retrovirology *9*, 53. https://doi.org/10.1186/1742-4690-9-53.
30. Goodier, J.L., Cheung, L.E., and Kazazian, H.H., Jr. (2012). MOV10 RNA helicase is a potent inhibitor of retrotransposition in cells. PLoS Genet. *8*, e1002941. https://doi.org/10.1371/journal.pgen.1002941.
31. Gregersen, L.H., Schueler, M., Munschauer, M., Mastrobuoni, G., Chen, W., Kempa, S., Dieterich, C., and Landthaler, M. (2014). MOV10 Is a 5′ to 3′ RNA helicase contributing to UPF1 mRNA target degradation by translocation along 3′ UTRs. Mol. Cell *54*, 573–585. https://doi.org/10.1016/j.molcel.2014.03.017.
32. Moldovan, J.B., and Moran, J.V. (2015). The Zinc-Finger Antiviral Protein ZAP Inhibits LINE and Alu Retrotransposition. PLoS Genet. *11*, e1005121. https://doi.org/10.1371/journal.pgen.1005121.
33. Li, X., Zhang, J., Jia, R., Cheng, V., Xu, X., Qiao, W., Guo, F., Liang, C., and Cen, S. (2013). The MOV10 helicase inhibits LINE-1 mobility. J. Biol. Chem. *288*, 21148–21160. https://doi.org/10.1074/jbc.M113.465856.
34. Hu, S., Li, J., Xu, F., Mei, S., Le Duff, Y., Yin, L., Pang, X., Cen, S., Jin, Q., Liang, C., and Guo, F. (2015). SAMHD1 Inhibits LINE-1 Retrotransposition by Promoting Stress Granule Formation. PLoS Genet. *11*, e1005367. https://doi.org/10.1371/journal.pgen.1005367.
35. Goodier, J.L., Pereira, G.C., Cheung, L.E., Rose, R.J., and Kazazian, H.H., Jr. (2015). The Broad-Spectrum Antiviral Protein ZAP Restricts Human Retrotransposition. PLoS Genet. *11*, e1005252. https://doi.org/10.1371/journal.pgen.1005252.
36. Li, M., Kao, E., Gao, X., Sandig, H., Limmer, K., Pavon-Eternod, M., Jones, T.E., Landry, S., Pan, T., Weitzman, M.D., and David, M. (2012). Codon-usage-based inhibition of HIV protein synthesis by human schlafen 11. Nature *491*, 125–128. https://doi.org/10.1038/nature11433.
37. van Zuylen, W.J., Garceau, V., Idris, A., Schroder, K., Irvine, K.M., Lattin, J.E., Ovchinnikov, D.A., Perkins, A.C., Cook, A.D., Hamilton, J.A., et al. (2011). Macrophage activation and differentiation signals regulate schlafen-4 gene expression: evidence for Schlafen-4 as a modulator of myelopoiesis. PLoS One *6*, e15723. https://doi.org/10.1371/journal.pone.0015723.
38. Liu, F., Zhou, P., Wang, Q., Zhang, M., and Li, D. (2018). The Schlafen family: complex roles in different cell types and virus replication. Cell Biol. Int. *42*, 2–8. https://doi.org/10.1002/cbin.10778.
39. Schwarz, D.A., Katayama, C.D., and Hedrick, S.M. (1998). Schlafen, a new family of growth regulatory genes that affect thymocyte development. Immunity *9*, 657–668.
40. Geserick, P., Kaiser, F., Klemm, U., Kaufmann, S.H.E., and Zerrahn, J. (2004). Modulation of T cell development and activation by novel members of the Schlafen (slfn) gene family harbouring an RNA helicase-like motif. Int. Immunol. *16*, 1535–1548. https://doi.org/10.1093/intimm/dxh155.
41. Brady, G., Boggan, L., Bowie, A., and O'Neill, L.A.J. (2005). Schlafen-1 causes a cell cycle arrest by inhibiting induction of cyclin D1. J. Biol. Chem. *280*, 30723–30734. https://doi.org/10.1074/jbc.M500435200.
42. Patel, V.B., Yu, Y., Das, J.K., Patel, B.B., and Majumdar, A.P.N. (2009). Schlafen-3: a novel regulator of intestinal differentiation. Biochem. Biophys. Res. Commun. *388*, 752–756. https://doi.org/10.1016/j.bbrc.2009.08.094.
43. Katsoulidis, E., Carayol, N., Woodard, J., Konieczna, I., Majchrzak-Kita, B., Jordan, A., Sassano, A., Eklund, E.A., Fish, E.N., and Platanias, L.C. (2009). Role of Schlafen 2 (SLFN2) in the generation of interferon alpha-induced growth inhibitory responses. J. Biol. Chem. *284*, 25051–25064. https://doi.org/10.1074/jbc.M109.030445.
44. Katsoulidis, E., Mavrommatis, E., Woodard, J., Shields, M.A., Sassano, A., Carayol, N., Sawicki, K.T., Munshi, H.G., and Platanias, L.C. (2010). Role of interferon {alpha} (IFN {alpha})-inducible Schlafen-5 in regulation of anchorage-independent growth and invasion of malignant melanoma cells. J. Biol. Chem. *285*, 40333–40341. https://doi.org/10.1074/jbc.M110.151076.
45. Oh, P.S., Patel, V.B., Sanders, M.A., Kanwar, S.S., Yu, Y., Nautiyal, J., Patel, B.B., and Majumdar, A.P.N. (2011). Schlafen-3 decreases cancer stem cell marker expression and autocrine/juxtacrine signaling in FOLFOX-resistant colon cancer cells. Am. J. Physiol. Gastrointest. Liver Physiol. *301*, G347–G355. https://doi.org/10.1152/ajpgi.00403.2010.
46. Mavrommatis, E., Arslan, A.D., Sassano, A., Hua, Y., Kroczynska, B., and Platanias, L.C. (2013). Expression and regulatory effects of murine Schlafen (Slfn) genes in malignant melanoma and renal cell carcinoma. J. Biol. Chem. *288*, 33006–33015. https://doi.org/10.1074/jbc.M113.460741.
47. Sassano, A., Mavrommatis, E., Arslan, A.D., Kroczynska, B., Beauchamp, E.M., Khuon, S., Chew, T.L., Green, K.J., Munshi, H.G., Verma, A.K., and Platanias, L.C. (2015). Human Schlafen 5 (SLFN5) Is a Regulator of Motility and Invasiveness of Renal Cell Carcinoma Cells. Mol. Cell Biol. *35*, 2684–2698. https://doi.org/10.1128/MCB.00019-15.
48. Yang, J.Y., Deng, X.Y., Li, Y.S., Ma, X.C., Feng, J.X., Yu, B., Chen, Y., Luo, Y.L., Wang, X., Chen, M.L., et al. (2018). Structure of Schlafen13 reveals a new class of tRNA/rRNA-targeting RNase engaged in translational control. Nat. Commun. *9*, 1165. https://doi.org/10.1038/s41467-018-03544-x.
49. Esnault, C., Maestre, J., and Heidmann, T. (2000). Human LINE retrotransposons generate processed pseudogenes. Nat.

Genet. *24*, 363–367. https://doi.org/10.1038/74184.

50. Walker, J.E., Saraste, M., Runswick, M.J., and Gay, N.J. (1982). Distantly related sequences in the alpha- and beta-subunits of ATP synthase, myosin, kinases and other ATP-requiring enzymes and a common nucleotide binding fold. EMBO J. *1*, 945–951.
51. Kopera, H.C., Flasch, D.A., Nakamura, M., Miyoshi, T., Doucet, A.J., and Moran, J.V. (2016). LEAP: L1 Element Amplification Protocol. Methods Mol. Biol. *1400*, 339–355. https://doi.org/10.1007/978-1-4939-3372-3_21.
52. Kulpa, D.A., and Moran, J.V. (2005). Ribonucleoprotein particle formation is necessary but not sufficient for LINE-1 retrotransposition. Hum. Mol. Genet. *14*, 3237–3248. https://doi.org/10.1093/hmg/ddi354.
53. Choi, J., Hwang, S.Y., and Ahn, K. (2018). Interplay between RNASEH2 and MOV10 controls LINE-1 retrotransposition. Nucleic Acids Res. *46*, 1912–1926. https://doi.org/10.1093/nar/gkx1312.
54. Lovsin, N., and Peterlin, B.M. (2009). APOBEC3 proteins inhibit LINE-1 retrotransposition in the absence of ORF1p binding. Ann. N. Y. Acad. Sci. *1178*, 268–275. https://doi.org/10.1111/j.1749-6632.2009.05006.x.
55. Warkocki, Z., Krawczyk, P.S., Adamska, D., Bijata, K., Garcia-Perez, J.L., and Dziembowski, A. (2018). Uridylation by TUT4/7 Restricts Retrotransposition of Human LINE-1s. Cell *174*, 1537–1548.e29. https://doi.org/10.1016/j.cell.2018.07.022.
56. Idica, A., Sevrioukov, E.A., Zisoulis, D.G., Hamdorf, M., Daugaard, I., Kadandale, P., and Pedersen, I.M. (2017). MicroRNA miR-128 represses LINE-1 (L1) retrotransposition by down-regulating the nuclear import factor TNPO1. J. Biol. Chem. *292*, 20494–20508. https://doi.org/10.1074/jbc.M117.807677.
57. Macia, A., Widmann, T.J., Heras, S.R., Ayllon, V., Sanchez, L., Benkaddour-Boumzaouad, M., Muñoz-Lopez, M., Rubio, A., Amador-Cubero, S., Blanco-Jimenez, E., et al. (2017). Engineered LINE-1 retrotransposition in nondividing human neurons. Genome Res. *27*, 335–348. https://doi.org/10.1101/gr.206805.116.
58. Freeman, B.T., Sokolowski, M., Roy-Engel, A.M., Smither, M.E., and Belancio, V.P. (2019). Identification of charged amino acids required for nuclear localization of human L1 ORF1 protein. Mob. DNA *10*, 20. https://doi.org/10.1186/s13100-019-0159-2.
59. Kubo, S., Seleme, M.D.C., Soifer, H.S., Perez, J.L.G., Moran, J.V., Kazazian, H.H., Jr., and Kasahara, N. (2006). L1 retrotransposition in nondividing and primary human somatic cells. Proc. Natl. Acad. Sci. USA *103*, 8036–8041. https://doi.org/10.1073/pnas.0601954103.
60. Mita, P., Wudzinska, A., Sun, X., Andrade, J., Nayak, S., Kahler, D.J., Badri, S., LaCava, J., Ueberheide, B., Yun, C.Y., et al. (2018). LINE-1 protein localization and functional dynamics during the cell cycle. Elife *7*, e30058. https://doi.org/10.7554/eLife.30058.
61. Shi, X., Seluanov, A., and Gorbunova, V. (2007). Cell divisions are required for L1 retrotransposition. Mol. Cell Biol. *27*, 1264–1270. https://doi.org/10.1128/MCB.01888-06.
62. Xie, Y., Mates, L., Ivics, Z., Izsvák, Z., Martin, S.L., and An, W. (2013). Cell division promotes efficient retrotransposition in a stable L1 reporter cell line. Mob. DNA *4*, 10. https://doi.org/10.1186/1759-8753-4-10.
63. Jankowsky, E. (2011). RNA helicases at work: binding and rearranging. Trends Biochem. Sci. *36*, 19–29. https://doi.org/10.1016/j.tibs.2010.07.008.
64. Metzner, F.J., Huber, E., Hopfner, K.P., and Lammens, K. (2022). Structural and biochemical characterization of human Schlafen 5. Nucleic Acids Res. *50*, 1147–1161. https://doi.org/10.1093/nar/gkab1278.
65. Neumann, B., Zhao, L., Murphy, K., and Gonda, T.J. (2008). Subcellular localization of the Schlafen protein family. Biochem. Biophys. Res. Commun. *370*, 62–66. https://doi.org/10.1016/j.bbrc.2008.03.032.
66. Belancio, V.P., Roy-Engel, A.M., Pochampally, R.R., and Deininger, P. (2010). Somatic expression of LINE-1 elements in human tissues. Nucleic Acids Res. *38*, 3909–3922. https://doi.org/10.1093/nar/gkq132.
67. Malouf, G.G., Monzon, F.A., Couturier, J., Molinié, V., Escudier, B., Camparo, P., Su, X., Yao, H., Tamboli, P., Lopez-Terrada, D., et al. (2013). Genomic heterogeneity of translocation renal cell carcinoma. Clin. Cancer Res. *19*, 4673–4684. https://doi.org/10.1158/1078-0432.CCR-12-3825.
68. Hoshimoto, S., Kuo, C.T., Chong, K.K., Takeshima, T.L., Takei, Y., Li, M.W., Huang, S.K., Sim, M.S., Morton, D.L., and Hoon, D.S.B. (2012). AIM1 and LINE-1 epigenetic aberrations in tumor and serum relate to melanoma progression and disease outcome. J. Invest. Dermatol. *132*, 1689–1697. https://doi.org/10.1038/jid.2012.36.
69. Tellez, C.S., Shen, L., Estécio, M.R.H., Jelinek, J., Gershenwald, J.E., and Issa, J.P.J. (2009). CpG island methylation profiling in human melanoma cell lines. Melanoma Res. *19*, 146–155.
70. Jones, R.B., Garrison, K.E., Wong, J.C., Duan, E.H., Nixon, D.F., and Ostrowski, M.A. (2008). Nucleoside analogue reverse transcriptase inhibitors differentially inhibit human LINE-1 retrotransposition. PLoS One *3*, e1547. https://doi.org/10.1371/journal.pone.0001547.
71. Carlini, F., Ridolfi, B., Molinari, A., Parisi, C., Bozzuto, G., Toccacieli, L., Formisano, G., De Orsi, D., Paradisi, S., Grober, O.M.V., et al. (2010). The reverse transcription inhibitor abacavir shows anticancer activity in prostate cancer cell lines. PLoS One *5*, e14221. https://doi.org/10.1371/journal.pone.0014221.
72. Sciamanna, I., Landriscina, M., Pittoggi, C., Quirino, M., Mearelli, C., Beraldi, R., Mattei, E., Serafino, A., Cassano, A., Sinibaldi-Vallebona, P., et al. (2005). Inhibition of endogenous reverse transcriptase antagonizes human tumor growth. Oncogene *24*, 3923–3931. https://doi.org/10.1038/sj.onc.1208562.
73. Mangiacasale, R., Pittoggi, C., Sciamanna, I., Careddu, A., Mattei, E., Lorenzini, R., Travaglini, L., Landriscina, M., Barone, C., Nervi, C., et al. (2003). Exposure of normal and transformed cells to nevirapine, a reverse transcriptase inhibitor, reduces cell growth and promotes differentiation. Oncogene *22*, 2750–2761. https://doi.org/10.1038/sj.onc.1206354.
74. Zhao, X., Zhao, Y., Du, J., Gao, P., and Zhao, K. (2021). The Interplay Among HIV, LINE-1, and the Interferon Signaling System. Front. Immunol. *12*, 732775. https://doi.org/10.3389/fimmu.2021.732775.
75. Dewannieux, M., Dupressoir, A., Harper, F., Pierron, G., and Heidmann, T. (2004). Identification of autonomous IAP LTR retrotransposons mobile in mammalian cells. Nat. Genet. *36*, 534–539. https://doi.org/10.1038/ng1353.
76. Schneider, C., Rasband, W., and Eliceiri, K. (2012). NIH Image to ImageJ: 25 years of image analysis. Nat Methods *9*, 671–675. https://doi.org/10.1038/nmeth.2089.
77. Sokolowski, M., DeFreece, C.B., Servant, G., Kines, K.J., deHaro, D.L., and Belancio, V.P. (2014). Development of a monoclonal antibody specific to the endonuclease domain of the human LINE-1 ORF2 protein. Mob. DNA *5*, 29. https://doi.org/10.1186/s13100-014-0029-x.
78. Van Meter, M., Kashyap, M., Rezazadeh, S., Geneva, A.J., Morello, T.D., Seluanov, A., and Gorbunova, V. (2014). SIRT6 represses LINE1 retrotransposons by ribosylating KAP1 but this repression fails with stress and age. Nat. Commun. *5*, 5011. https://doi.org/10.1038/ncomms6011.

STAR★METHODS

KEY RESOURCES TABLE

REAGENT or RESOURCE	SOURCE	IDENTIFIER
Antibodies		
Monoclonal anti-Flag M2 antibody	Sigma-Aldrich	Cat:#F3165; RRID:AB_259529
Rabbit monoclonal [EPR20018-251] to DDDDK tag	abcam	Cat:#ab205606; RRID:AB_2916341
Goat polyclonal to DDDDK tag (Binds to FLAG® tag sequence)	abcam	Cat:#ab1257; RRID:AB_299216
Monoclonal Anti-c-Myc antibody produced in mouse	Sigma-Aldrich	Cat:#M4439; RRID:AB_439694
Anti-C-Myc antibody produced in rabbit	Sigma-Aldrich	Cat:#C3956; RRID:AB_439680
anti-SLFN5 antibody	abcam	Cat:#ab121537; RRID:AB_11130104
Anti-ORF2 antibody	Abmart	N/A
Mouse monoclonal [mAbcam 8226] to beta Actin	abcam	Cat:#ab8226; RRID:AB_306371
Anti-ORF1 antibody	Gift from Dr. Fei Guo	N/A
Anti-S9.6 antibody	abcam	Cat:#ab234957
Alexa Fluor 647 anti-mouse antibody	Life technologies	Cat:#A21447
FITC anti-rabbit antibody	Transgene	Cat:#HS211
Chemicals, peptides, and recombinant proteins		
RNase A	ThermoFisher	Cat:#EN0531
Lipofectamine 2000	Thermo Fisher Scientific	Cat:#11668019
Lipofectamine RNAiMAX	Thermo Fisher Scientific	Cat:#13778150
Geneticin (G418)	absin	Cat:#abs812846
DNase	Takara	Cat:#2270A
RNasin	Promega	Cat:#N2115
Recombinant RNase inhibitor	Takara	Cat:#2313A
RNase H	New England BioLabs	Cat:#M0297L
Dynabeads Protein A	Invitrogen	Cat:#10002D
Critical commercial assays		
Sso Fast Eva Green Supermix	BioRad	Cat:#1725202
Minute Cytosolic and Nuclear Extraction kit	Invent Biotechnologies	Cat:#NT-032
RNAscope® Multiplex Fluorescent Reagent Kit v2 Assay	Advanced Cell Diagnostics	Cat. No. 323110
RNAscope™ Probe- Hs-LINE1-ORF2-sense	Advanced Cell Diagnostics	Cat:#523251
Experimental models: Cell lines		
HEK293T	ATCC	Cat:#CRL-11268; RRID:CVCL_1926
HeLa	ATCC	Cat:#CCL-2; RRID:CVCL_0030
Oligonucleotides		
Primer: wild SLFN5 Forward: 5′ ATAGGTACCGCCACCATG AGTCTTAGGATTGATG 3′	This paper	N/A
Primer: wild SLFN5 Reverse: 5′ ATA CCGCGGCACAGAA GCCTTCA GAATATACAGA 3′	This paper	N/A
Primer: dC1 Reverse: 5′ ATACCGCGGGAGAAAAC GGCATTTATTCGC TAC 3′	This paper	N/A

(*Continued on next page*)

Continued

REAGENT or RESOURCE	SOURCE	IDENTIFIER
Primer: dC2 Reverse: 5′ ATACCGCGGCTTGCGAA GGTTCTTTGAAAGCAAC 3′	This paper	N/A
Primer: dC3 Reverse: 5′ ATA CCGCGGAGCTTCC ATCATCCAAGCAGTCCAT 3′	This paper	N/A
Primer: dN1 Forward: 5′ ATAGGTACCGCCACCATG AATTCATTAGGTCCAC 3′	This paper	N/A
5′ Primer: dN2 Forward: ATAGGTACCGCCACCATGG CTGACCCAGACCTTT3′	This paper	N/A
Primer: dN3 Forward: 5′ ATAGGTACCGCCACCAT GATTCTCTACACCATCT 3′	This paper	N/A
sgRNA targeting sequence: *SLFN5 sense*: CACCGTAGAA GCCCTCAAGCTCGTA	This paper	N/A
sgRNA targeting sequence: *SLFN5 antisense*: AAACTACG AGCTTGAGGGCTTCTAC	This paper	N/A
Primer: L1 Forward: 5′-AATGAGATCACATGGA CACAGGAAG-3′	This paper	N/A
Primer: L1 Reverse: 5′- TGTATACATGTGCCAT GCTGGTGC-3′	This paper	N/A
Primer for RT-PCR:GAPDH Forward: TGACGTGGACATCCGCAAAG	This paper	N/A
Primer for RT-PCR:GAPDH Forward: 5′- GGTATCGTGGAAGGACTCATGAC-3′	This paper	N/A
Primer for RT-PCR:GAPDH Reverse: 5′-ATGCCAGTGAGCTTCCCGTTCAG-3′	This paper	N/A
Primer for L1 cDNA Forward: 5′-AGTTCGGCTGGCGCGAGGCCC-3′	This paper	N/A
Primer for L1 cDNA Reverse: 5′-CTGAAGCGGGAAGGGACTG-3′	This paper	N/A
3′ RACE adapter primer: 5′- GCGAGCACAGAATTAATACG ACTCACTATAGGTTTTTTTTTTVN-3′	This paper	N/A
Primer for MDM2 Forward: 5′- AGCTTGGCTGCTTCTGGG-3′	This paper	N/A
Primer for MDM2 Reverse: 5′- GTACGCACTAATCCGGGGAG-3′	This paper	N/A
Recombinant DNA		
Plasmid: 5′UTR-L1-neoRT	This paper	N/A
Plasmid: CMV-L1-neo^{RT}(D702Y)	This paper	N/A
Plasmid: MusD-neo^{TNF}	Dewannieux et al.[75]	N/A
Plasmid: SLFN5-Flag	This paper	N/A

(*Continued on next page*)

Continued

REAGENT or RESOURCE	SOURCE	IDENTIFIER
Plasmid: SLFN5-Myc	This paper	N/A
Plasmid: SLFN5 (K584R)	This paper	N/A
Plasmid: SLFN5 (D649A)	This paper	N/A
Plasmid: SLFN5 (K584R/D649A)	This paper	N/A
Plasmid: dN1(Δ1-150aa)	This paper	N/A
Plasmid: dN2(Δ1-335aa)	This paper	N/A
Plasmid: dN3(Δ1-450aa)	This paper	N/A
Plasmid: dC1(Δ781-891aa)	This paper	N/A
Plasmid: dC2(Δ571-891aa)	This paper	N/A
Plasmid: dC3(Δ335-891aa)	This paper	N/A
Plasmid: pET28a-ORF2p-EN(1-239aa)	This paper	N/A
Plasmid: IAP-neo^{TNF}	This paper	N/A
Software and algorithms		
Image J	Schneider et al., 2012[76]	https://imagej.nih.gov/ij/
GraphPad Prism 8	GraphPad software	N/A

RESOURCE AVAILABILITY

Lead contact

Further information and requests for resources should be directed to and will be fulfilled by the lead contact, Xiaoyu Li (lixiaoyu@imb.pumc.edu.cn).

Materials availability

Plasmids and cell lines generated in this study will be available upon request from the lead contact.

Data and code availability

- The data reported in this paper will be shared upon request to the lead corresponding author (lixiaoyu@imb.pumc.edu.cn).
- This paper does not report original code.
- Any additional information required to reanalyze the data reported in this paper is available from the lead contact upon request.

EXPERIMENTAL MODEL AND STUDY PARTICIPANT DETAILS

Cell lines

Human embryonic kidney HEK-293T cells and HeLa cells were grown at 37°C in Dulbecco's modified Eagle's medium (DMEM) supplemented with 10% foetal bovine serum (Gibco) in a humidified incubator in 5% CO_2. SLFN5 knockout HeLa cells were generated by the CRISPR–Cas9 system. Briefly, HeLa cells were transfected with the pLentiCRISPR v.2 vector (Addgene) encoding 5 independent sgRNAs targeting SLFN5 and a scramble sgRNA (negative control). Transfected HeLa cells were then grown in 2 μg/mL puromycin and split 1:5 once the cell density reached 80%–90% confluence. Cells were grown over 2 passages with the selection medium. The survived clones were selected and expanded. Knockout of the SLFN5 gene for each cell clone was confirmed by immunoblotting using an anti-SLFN5 antibody (Abcam) and then named SLFN5-KO-HeLa.

METHOD DETAILS

Plasmids and antibodies

CMV-L1-neo^{RT} contains a complete human LINE-1 DNA copy that has a neomycin resistance gene inserted just before the 3′-UTR of LINE-1 in the opposite direction from the LINE-1 coding sequence.[49] The MusD-neo^{TNF} plasmid expressing mouse LTR retrotransposons contains a similar neomycin resistance cassette placed in the reverse direction.[75] The neomycin resistance gene is inactivated by the presence of a forward intron that can be removed during RNA splicing, thus producing a functional neomycin resistance gene after reverse transcription and integration. The pcDNA4.0-based SLFN5 DNA clone encodes a C-terminal Flag-tagged human SLFN5 protein. Three SLFN5 mutants, SLFN5 (K584R), SLFN5 (D649A) and SLFN5 (K584R/D649A), which have the amino acids Lys-584 and/or Asp-649 mutated to Arg and Ala, respectively, were constructed using a site-directed mutagenesis kit (Stratagene). The LINE-1 promoter reporter plasmid L1-FL, which contains a 670-nt LINE-1 5′-UTR sequence in the pGL3-Basic vector (Promega), was described previously.[33] Lipofectamine 2000 (Invitrogen) was used for transient transfection.

SLFN5 deletion constructs including full-length, N-terminal and C-terminal truncations (dN1(Δ1-150aa), dN2(Δ1-335aa), dN3(Δ1-450aa), dC1(Δ781-891aa), dC2(Δ571-891aa) and dC3(Δ335-891aa) were individually cloned into pDNA4-myc vector via KpnI and SacII restriction sites. We used the following primers: wild-type: 5′ ATAGGTACCGCCACCATG AGTCTTAGGATTGATG 3′ (forward primer) and 5′ ATA CCGCGGCACAGAAGCCTTCA GAATATACAGA 3′ (reverse primer); Cd1 5′ ATACCGCGGGAGAAAACGGCATTTATTCGC TAC 3′ (reverse primer); Cd2: 5′ ATACCGCGGCTTGCGAAGGTTCTTTGAAAGCAAC 3′ (reverse primer); Cd3: 5′ ATA CCGCGGAGCTTCCATCATCC AAGCAGTCCAT 3′ (reverse primer); Nd1: 5′ ATAGGTACCGCCACCATGAATTCATTAGGTCCAC 3′ (forward primer); Nd2 5′ ATAGGT ACCGCCACCATGGCTGACCCAGACCTTT3′ (forward primer); Nd3: 5′ ATAGGTACCGCCACCATGATTCTCTACACCATCT 3′ (forward primer).

Anti-Flag antibody (mouse) and anti-β-actin antibody (mouse) were purchased from Sigma–Aldrich, and anti-SLFN5 antibody (rabbit) was purchased from Abcam. The ORF1p antibody (rabbit) was a gift from Dr. Guo's laboratory.[34]

The cDNA of the ORF2p endonuclease (EN) domain (residues 1–239)[77] was amplified by PCR and cloned into the expression vector pET28a (Novagene, Germany). The recombinant ORF2p EN domain with N-terminal poly-histidine tag was expressed in *Escherichia coli* Rosetta II cells (Novagen) after induction with IPTG and purified using Ni-NTA resin (QIAGEN) following the instructions from the manufacturer. The purified protein was provided to the company (Abmart, Inc.) for immunizing rabbits to produce ORF2p antibody. The purified antibody was tested for their recognition of ORF2p by Western blotting and immunofluorescence staining.

Retrotransposition assay

HeLa cells were seeded in 35 mm tissue culture dishes 1 day prior to transfection. The next day, cells were cotransfected with 1000 ng of CMV-L1-neo^{RT}, MusD-neo^{TNF}, IAP-neo^{TNF} or pcDNA3.1 DNA with 500 ng SLFN5 DNA. Forty-eight hours later, cells were detached from the plates with trypsin and seeded into 35 mm tissue culture dishes at the cell density of 1x10^5/dish. Plasmid pcDNA3.1 (Invitrogen), which carries an intact neomycin resistance gene, served as a control for the specificity of SLFN5 inhibition. G418 (0.4 mg/mL) was then added to select for resistant cell colonies. After 10–12 days of selection, when cell colonies were clearly visible, the cells were fixed with methanol for 10 min and stained with 0.5% crystal violet (in 25% methanol) for 10 min. The number of colonies represents the transposition efficiency of LINE-1.

Quantification of LINE-1 RNA by RT–qPCR

HeLa cells were transfected with CMV-L1-neo^{RT} reporter DNA with or without SLFN5 DNA. Forty-eight hours later, total RNA was extracted by TRIzol reagents (Invitrogen). cDNA was synthesized by Moloney murine leukemia virus (MLV) RT (Takara), followed by DNase treatment (Takara). cDNA was quantified by qPCR kits (Sso Fast Eva Green Supermix, Takara) using primers (5′-AATGAGATCACATGGACACAG GAAG-3′/5′- TGTATACATGTGCCATGCTGGTGC-3′).[78]

Quantification of reverse transcribed LINE-1 DNA by qPCR

HeLa cells were transfected with the CMV-L1-neo^{RT} plasmid with or without SLFN5 DNA. Seventy-two hours after transfection, total cellular DNA was extracted with the QIAamp DNA Mini kit (QIAGEN). Equal amounts of DNA templates (250 ng) were subjected to PCR with primers 5′-AGTTCGGCTGGCGCGAGGCCC-3′/5′-CTGAAGCGGGAAGGGACTG-3′, which were used to amplify LINE-1 cDNA reverse transcribed from LINE-1 RNA. The forwards primer spans the exon/intron junction within the neomycin resistance gene such that only the spliced and reverse transcribed DNA can be amplified. Levels of GAPDH DNA were detected as an internal control to normalize the amount of LINE-1 DNA using the primers 5′-GGTATCGTGGAAGGACTCATGAC-3′/5′-ATGCCAGTGAGCTTCCCGTTCAG-3′.

Cell nuclear and cytoplasmic extraction

Cells were isolated using the Minute Cytosolic and Nuclear Extraction kit (Invent Biotechnologies, Eden Prairie, MN) according to the manufacturer's instructions. Briefly, cells per well were lysed in 300 μL of cytoplasmic extraction buffer in 6-well plates and collected in a 1.5-mL microcentrifuge tube. After vortexing for 15 s, the tube was incubated on ice for 5 min followed by centrifugation at 14000 rpm for 10 min. The supernatant was kept as cytosolic components, and 100 μL of nuclear extraction buffer was added to the pellet. After 5 repeated steps of vortexing and incubation on ice, the nuclear extracts were isolated by centrifugation at 14000 rpm for 30 s in a collection tube through a filter cartridge.

Western blotting

Cells were lysed with NP-40 buffer (Beyotime). Equal amounts of cell lysates were separated by 10% SDS–PAGE. Proteins were transferred onto a PVDF membrane, blocked with 5% skim milk, and probed with primary antibodies, including anti-Flag antibody (diluted 1:5000), anti-SLFN5 antibody (diluted 1:1000), or anti-β-actin antibody (diluted 1:5000), at 4°C overnight. After four wash steps with PBS plus 0.1% Tween 20 (PBST), the membrane was incubated with a 1:5000 dilution of HRP-conjugated goat-anti-mouse secondary antibody for 1 h at room temperature. After four wash steps with PBS plus 0.1% Tween 20 (PBST), signals were detected using Western Lighting chemiluminescence reagent.

Proteins that needed to be quantified were acquired using the Odyssey infrared imaging system. After primary antibody incubation and membrane washing, membranes were incubated with fluorescent secondary antibody and then incubated for 1 h in a dark chamber at room temperature. Images were analyzed with the Odyssey infrared imaging system following the operating manual.

LINE-1 element amplification protocol (LEAP)

The LEAP assay was carried out as previously described.[3,51] Briefly, HeLa cells were seeded in T-75 flasks and transfected with CMV-L1-neo^{RT} reporter DNA and SLFN5 plasmid. Forty-eight hours later, the cells were harvested and lysed, and the cleared whole cell lysates were centrifuged through an 8.5%/17% (w/v) sucrose cushion at 178,000 g for 2 h. The resultant pellet was resuspended in 100 μL Tris buffer (2 mM pH 8.0 Tris. HCl, 1X Complete EDTA-free protease inhibitor cocktail, Roche). The total protein concentration was determined by a Bradford assay following standard protocols, and an Odyssey infrared imaging system was used to adjust the amount of RNP using anti-ORF2p antibodies. An aliquot of the RNP sample was added to 49 μL of LEAP assay master mix (50 mM Tris. HCl (pH 7.5), 50 mM KCl, 5 mM $MgCl_2$, 10 mM DTT, 0.4 mM 3′ RACE adapter primer (5′-GCGAGCACAGAATTAATACGACTCACTATAGGTTTTTTTTTTVN-3′), 20 U RNasin (Promega), 0.2 mM dNTPs, and 0.05% (v/v) Tween 20) and incubated at 37°C for 1 h. The LEAP cDNA product levels were quantified by real-time PCR (Sso Fast Eva Green Supermix, Takara) using the following primers as previously described: (5′- AATGAGATCACATGGACACAGGAAG-3′/5′-TGT ATACATGTGCCATGCTGGTGC -3′).[78] The copy number of LINE-1 RNA was calculated by generating a standard curve using serial dilutions of CMV-L1-neo^{RT} reporter DNA.

Co-Immunoprecipitation (CoIP) assay

HEK293 cells were cotransfected with SLFN5 and CMV-L1-neo^{RT} DNA. The cells were collected 48 h posttransfection and then lysed in 350 μL of TNT buffer (20 mM Tris. HCl, pH 7.5, 200 mM NaCl, 1% Triton X-100). Insoluble material was pelleted at 1800 x g for 30 min. Equal amounts of supernatant were incubated with 5 μL of anti-Flag antibody or anti-ORF1p antibody for 16 h at 4°C, followed by the addition of protein A-Sepharose (Amersham Biosciences) for 2 h. The immunoprecipitated complex was then washed three times with TNT buffer and phosphate-buffered saline, followed by Western blot analysis using anti-Flag or anti-ORF1p antibodies, respectively.

RNA immunoprecipitation (RIP)

HEK293 cells were transfected with 1000 ng CMV-L1-neo^{RT} with 500 ng SLFN5 and its mutant DNA. The cells were collected 48 h posttransfection and then lysed in 350 μL of TNT buffer (20 mM Tris. HCl, pH 7.5, 200 mM NaCl, 1% Triton X-100) with RNase inhibitor (Takara) at a final concentration of 1 U/μl. The expressed ORF1p or SLFN5 was immunoprecipitated with anti-ORF1p or anti-Myc antibody as described above. The RNA associated with the precipitated complex was extracted with TRIzol agents (Invitrogen) and subjected to RT–PCR using primers that amplify the *Neo* gene as described above.

RNA fluorescence *in situ* hybridization (FISH)

LINE-1 RNA in HeLa cells was measured by RNAscope assay (Advanced Cell Diagnostics, ACD, Hayward, CA) following the manufacturer's instructions. In brief, HeLa cells were seeded into four-chamber slides 1 day prior to transfection with 200 ng CMV-L1-neo^{RT} and 200 ng SLFN5-Flag or empty vector. Then, the cells were fixed with 4% paraformaldehyde (in 1x phosphate-buffered saline) for 20 min at room temperature followed by treatment with RNAscope Protease Plus for 15 min. Cells were then hybridized with RNA probes (Hs-LINE-1 ORF2, purchased from ACD, Inc), and signal amplification steps were performed according to the manufacturer's instructions before incubation with anti-Flag antibodies and secondary antibodies to stain the SLFN5 protein. Finally, cells were mounted with mounting oil containing DAPI and observed under an Olympus IX81 confocal microscope using a 100x immersion lens (NA 1.35) for imaging.

RNA-DNA hybrid immunoprecipitation (DRIP)

DRIP was performed as described previously with the following modifications.[53] Briefly, HeLa cells were lysed with lysis buffer (10 mM Tris-HCl pH 8.0, 100 mM NaCl, 25 mM EDTA pH 8.0, 0.5% SDS, 10 μg/mL Proteinase K) and incubated overnight at 55°C. Total nucleic acids were extracted using the standard phenol–chloroform extraction method and resuspended in TE buffer. The nucleic acids were digested with a restriction enzyme cocktail (20 units of EcoRI, BamHI, HindIII, BsrBI and XhoI; New England BioLabs) overnight at 37°C. The digested nucleic acids were subsequently used for qPCRs. As a negative control, half of the sample was treated with 10 units of RNase H (New England BioLabs) overnight at 37°C. The resulting fragmented DNA samples were isolated using the phenol–chloroform extraction method and resuspended in TE buffer. RNA-DNA hybrids were immunoprecipitated from total nucleic acids by adding 10 μg of S9.6 antibody (Abcam) in IP buffer (10 mM Na_3PO4 pH 7.0, 140 mM NaCl, 0.05% Triton X-100) and incubated overnight at 4°C. Dynabeads Protein A (50 μL; Invitrogen) was used to pull down the DNA-antibody complexes. The beads were incubated with the samples at room temperature for 3 h and then washed three times with IP buffer. The DNA was eluted with IP buffer and treated for 1 h with 10 μL of proteinase K (10 μg/mL) at 55°C. Additionally, RNase A was added and incubated with the samples for 1 h at 37°C to degrade RNA. Subsequently, DNA was purified following the phenol–chloroform extract method. The relative abundances of immunoprecipitated RNA-DNA hybrids at the indicated region were calculated as follows: $\Delta Ct = 2(\Delta Ct^{Input} - \Delta Ct^{IP})$. Nucleic acid enrichment was further normalized to a control primer pair specific to *MDM2*, a protein that binds DNA-RNA hybrids in the DNA damage response, and calculated using the equation $\Delta\Delta Ct = \Delta Ct^{experiment}/\Delta Ct^{control}$. Student's *t* test was used to assess statistical significance.

Discontinuous sucrose gradient ultracentrifugation

HEK293T cells were transfected with LINE-1 DNA and wild-type or mutant SLFN5 constructs. Seventy-two hours later, cells (5.4×10^7) were washed with PBS and lysed with 1 mL NP-40 buffer with RNase inhibitor (Takara) at a final concentration of 1 U/μl. The cell lysates were

centrifuged at 12000 rpm (10 min) to remove the cell debris. The samples were prepared into 2 mL solutions containing 10 mM Tris-HCl (pH 8.0), 1 mM EDTA, 150 mM NaCl and 5% (w/v) sucrose. Two millilitres of 50% (w/v) sucrose were placed at the bottom of ultracentrifuge tubes, followed by 2 mL 35% (w/v) sucrose, 2 mL 20% (w/v) sucrose, 2 mL sample in 5% (w/v) sucrose, 2 mL 5% (w/v) sucrose, 1 mL 10 mM Tris HCl (pH 8.0), and 1 mM EDTA buffer without sucrose. The samples were centrifuged at 160 000 g (SW41 rotor, Beckman) for 4 h. Forty fractions of each sample were collected from top to bottom, followed by Western blot and RT–qPCR analyses.

QUANTIFICATION AND STATISTICAL ANALYSIS

All experiments were repeated at least 3 independent times otherwise stated in the figure legends. The replicate number, mean, and error bars are explained in the figure legends. The statistical tests we used and resulting p values are indicated in the figure panels and/or figure legends. Statistical analyses were performed using GraphPad Prism 8.0 software.